ALPHA TAXONOMY OF EOCENE PRIMATES FROM THE GREAT DIVIDE BASIN, WYOMING

By

Dakota R. Pavell

July 2021

Director of Thesis: James E. Loudon

Major Department: Anthropology

The identification of the alpha taxonomy of an extinct species is the first step towards understanding its evolutionary history. The alpha taxonomy refers to the initial classification of the specimen based on the analysis of the observable morphological traits. Many paleoprimatologists, paleobiologists, and paleoanthropologists in the past have conducted these morphological examinations via visible observations or with the use of a microscope. As technology advances, new methods have been introduced that have changed the process of these morphological examinations. I examined eleven specimens that have been previously identified as primate teeth from the Eocene Epoch (~55-41 mya) using a micro computed tomography (CT) scanner located at the Shared Materials and Instrumentation Facility at Duke University. The projections of the specimens taken from the micro CT scanner were imported into Avizo, a three-dimensional visualization software, to generate digital reconstructions. The digital reconstructions were used for further morphological analyses to aid in the identification of the taxonomic classifications of the study specimens. Ten of the specimens were classified into the genus *Cantius*, the stem genus for a group of lemur-like primates known as the Nothartcine

primates. One of the specimens was classified into the genus *Copelemur*, another Notharctine primate genus. The study specimens were classified through the combination of observable dental morphology and molar measurements. Given the similarities between the study specimens and modern Malagasy lemurs, a brief comparison of dental morphology is also provided. The data generated here demonstrate that the alpha taxonomy of a specimen can be identified based on the evidence provided in the digital reconstructions, therefore, this process can be used to further our understanding of the fossil record.

ALPHA TAXONOMY OF EOCENE PRIMATES FROM THE GREAT DIVIDE BASIN, WYOMING

A Thesis

A Thesis Presented to the Faculty of the Department of Anthropology

East Carolina University

In Partial Fulfillment of the Requirements for the Degree

Master of Arts in Anthropology

By

Dakota R. Pavell

July 2021

ALPHA TAXONOMY OF EOCENE PRIMATES FROM THE GREAT DIVIDE BASIN, WYOMING

By

Dakota Pavell

APPROVED BY:

DIRECTOR OF THESIS: _____
James E. Loudon, PhD

COMMITTEE MEMBER: _____
Robert L. Anemone, PhD

COMMITTEE MEMBER: _____
Megan Perry, PhD

COMMITTEE MEMBER: _____
Ryan Schacht, PhD

CHAIR OF THE DEPARTMENT OF ANTHROPOLOGY: _____
I. Randolph Daniel, PhD

DEAN OF THE GRADUATE SCHOOL: _____
Paul J. Gemperline, PhD

ACKNOWLEDGMENTS

I would like to thank my advisor Dr. James E. Loudon for his guidance, enthusiasm, and the constant support he provided for this project. His assistance was greatly appreciated, and necessary for my successful completion. Additionally, I would like to thank Dr. Robert L. Anemone for providing the fossils used for scanning and the training he provided that was vital to the completion of this project. All the fossils described here were collected on federal land under BLM Permit 287-WY-PA95 by field crews under the direction of Dr. Anemone. This project would not have been possible without his assistance. I would also like to thank Justin Gladman at the Shared Materials and Instrumentation Facility located at Duke University for providing me with the necessary training required to work with the micro computed tomography (CT) scanner and with Avizo Lite. Justin's help was essential, and I am grateful. I would also like to thank my thesis committee members, Dr. Megan Perry and Dr. Ryan Schacht, for their advice and assistance with the revisions of the written aspects associated with this project. I would also like to thank Nathan Bianco for his assistance with the statistical analyses provided in this document. Finally, I would like to thank the Research Triangle Nanotechnology Network (RTNN) for providing funding for this project through the Kickstarter Program and I would also like to thank the East Carolina University Graduate School for providing summer funding for this project.

TABLE OF CONTENTS

LIST OF TABLES

LIST OF FIGURES

13. Lateral Surface of CM 95511, a *C. trigonodus* specimen with $M_2 – M_3$. Mesial to the right of the page.

14. Occlusal Surface of CM 95511, *C. trigonodus* specimen with $M_2 – M_3$. Mesial to the right of the page; buccal to the bottom of the page.
15. Lateral Surface of CM 95512, a *C. trigonodus* specimen with M_3. Mesial to the right of the page.
16. Occlusal Surface of CM 95512, a *C. trigonodus* specimen with M_3. Mesial to the right of the page; buccal to the bottom of the page.
17. Occlusal Surface of CM 95513, a *C. trigonodus* specimen with $P^3 – M^3$. Mesial to the right of the page; buccal to the top of the page.
18. Lateral Surface of CM 95514, a *C. frugivorous* specimen with $P_4 – M_1$. Mesial to the right of the page.
19. Occlusal Surface of CM 95514, a *C. frugivorous* specimen with $P_4 – M_1$. Mesial to the right of the page; buccal to the bottom of the page.
20. Lateral Surface of CM 95514, a *C. frugivorous* specimen with $M_1 – M_2$. Mesial to the right of the page.
21. Occlusal Surface of CM 95515, a *C. frugivorous* specimen with $M_1 – M_2$. Mesial to the right of the page; buccal to the bottom of the page.
22. Lateral Surface of CM 95516, a *C. frugivorous* specimen with $P_3 – M_3$. Mesial to the right of the page.
23. Occlusal Surface of CM 95516, a *C. frugivorous* specimen with $P_3 – M_3$. Mesial to the right of the page; buccal to the bottom of the page.

24. Occlusal Surface of CM 95517, a *C. trigonodus* specimen with M^2-M^3. Mesial to the right of the page; buccal to the top of the page.
25. Lateral Surface of CM 95509, a *Copelemur australotutus* specimen with P_3 – M_1. Mesial to the left of the page.
26. Occlusal Surface of CM 95509, a *Copelemur australotutus* specimen with P_3 – M_1. Mesial to the left of the page; buccal to the bottom of the page.

Chapter 1

Introduction

Taxonomy is the classification of life. Throughout history, humans have informally classified the species they live among to make sense of their worlds. One of the earliest formal taxonomic systems was developed by Aristotle, who classified organisms as plants or animals based on their physical attributes (Mayr, 1982). Existing models were revolutionized by the Swedish botanist Carolus Linnaeus who devised a hierarchical taxonomic system in his multiple volumes of the *Systema Naturae* (Wilson, 2010). Linnaeus utilized a standardized system that included two names, referred to as the binomial nomenclature. Although vastly expanded upon, the Linnaean system is still used by modern taxonomists. The Linnaean taxonomic system can also be employed to classify extinct species (Mayr, 1963). Although the fossil record is inherently discontinuous and fragmented, understanding of the taxonomic groups of extinct species provides a context for interpreting those species that exist today.

The primary goal of this project is to improve our understanding of the taxonomy of *Cantius*, an extinct genus of primates that once inhabited the western regions of North America. Dental morphological traits of *Cantius* were examined using a micro computed tomography (CT) scanner and three-dimensional reconstructions generated by Avizo, a visualization software program developed to study the morphological and structural characteristics of elements. Dental morphological traits generated from these scans were combined with length and width measurements of *Cantius* molars to examine the variation of the teeth among the *Cantius* specimens. This study focuses on the occlusal molar surfaces of

eleven specimens and aims to identify the presence of the definitive morphological characteristics that are expected to belong to the genus *Cantius*. The dental morphological traits of the *Canitus* specimens examined in this study were compared to the characteristics of other extinct North American primates referred to as the Notharctine primates.

Notharctine primates

The Notharctine primates consists of five primary genera: *Notharctus, Pelycodus, Copelemur, Smilodectes*, and *Cantius*. The Notharctine primates were one of the most common groups of mammals among the early and middle Eocene faunas in North America. Of the five genera, the early species of *Cantius* appear to have the most primitive dental morphology (Beard, 1988; Covert, 1990). The gradual evolution of the *Cantius* species has been a topic of interest for many paleoprimatologists given that they are among the most common of the Notharctine primates, and comparatively, the specimens of this genus have been recovered over a large geographic distribution (Beard, 1988). This project focuses on the alpha taxonomy of ten *Cantius* specimens, and one additional *Copelemur* specimen for comparison. The term alpha taxonomy refers to the initial identification of a specimen based on a morphological examination done in order to determine the taxonomic classification of the specimen (Turrill, 1935).

Among the Notharctine primates, fossilized dental remains recovered from dated strata suggest that *Copelemur* and *Pelycodus* were the next genera to evolve. All three of these genera, *Cantius, Copelemur*, and *Pelycodus* evolved during the Wasatchian North American Land Mammal Age (NALMA) and have been recovered in the western regions of North America, primarily in Wyoming, New Mexico, and Colorado with a few outliers in North

Dakota and California (Figure 1) (Covert, 1990; Woodbourne, et. al., 2009). The remaining two genera include *Notharctus* and *Smilodectes*, which were the last of the genera to appear in the fossil record and lived during the mid-Eocene, within the Bridgerian North American Land Mammal Age (NALMA). Fossils of *Notharctus* and *Smilodectes* have be recovered primarily in Wyoming and New Mexico with a few outliers in Texas, Utah, and Colorado (Figure 2) (Covert, 1990).

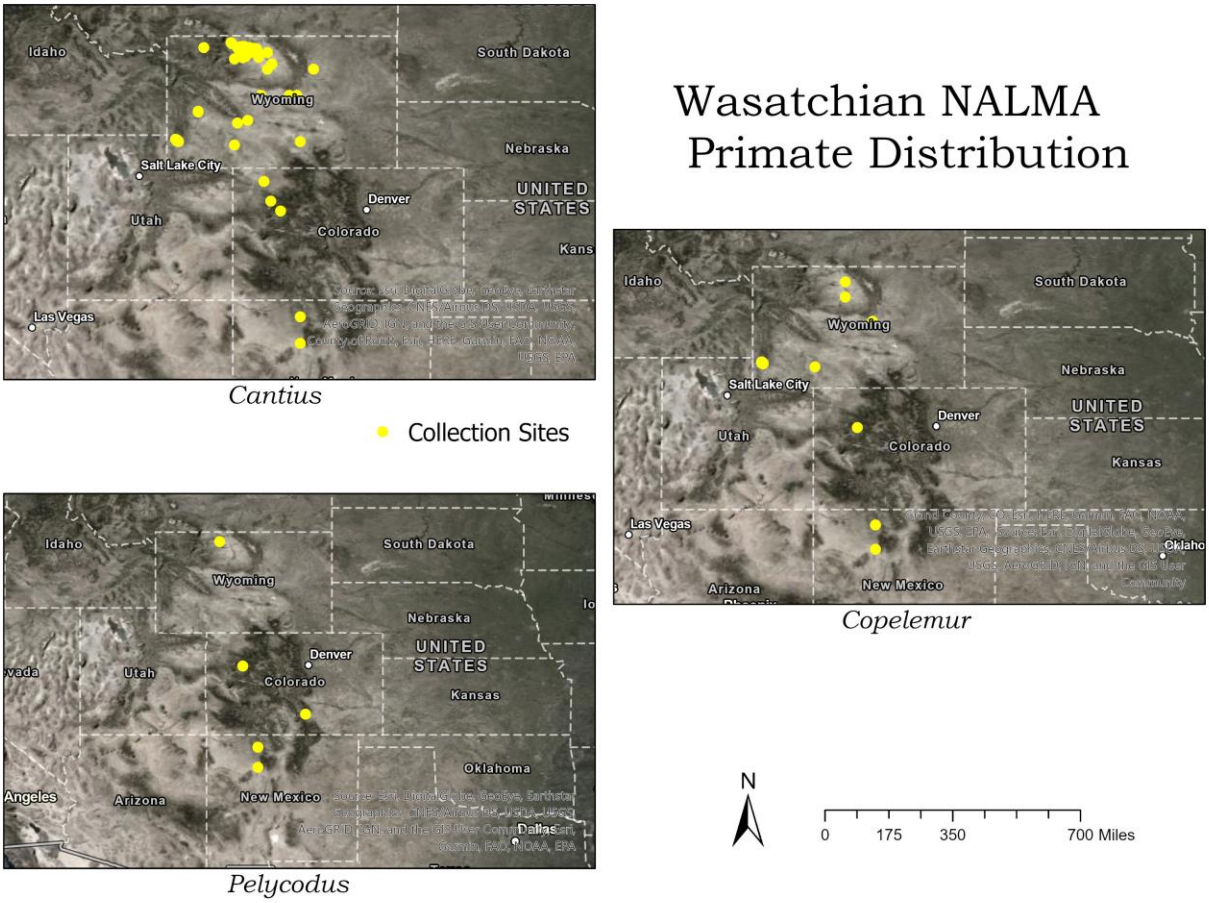

Figure 1. Geographic distribution of the Wasatchian Notharctine primates based on the location of the collection sites. Collection Sites: Paleobiology Database (https://paleobiodb.org/#/).

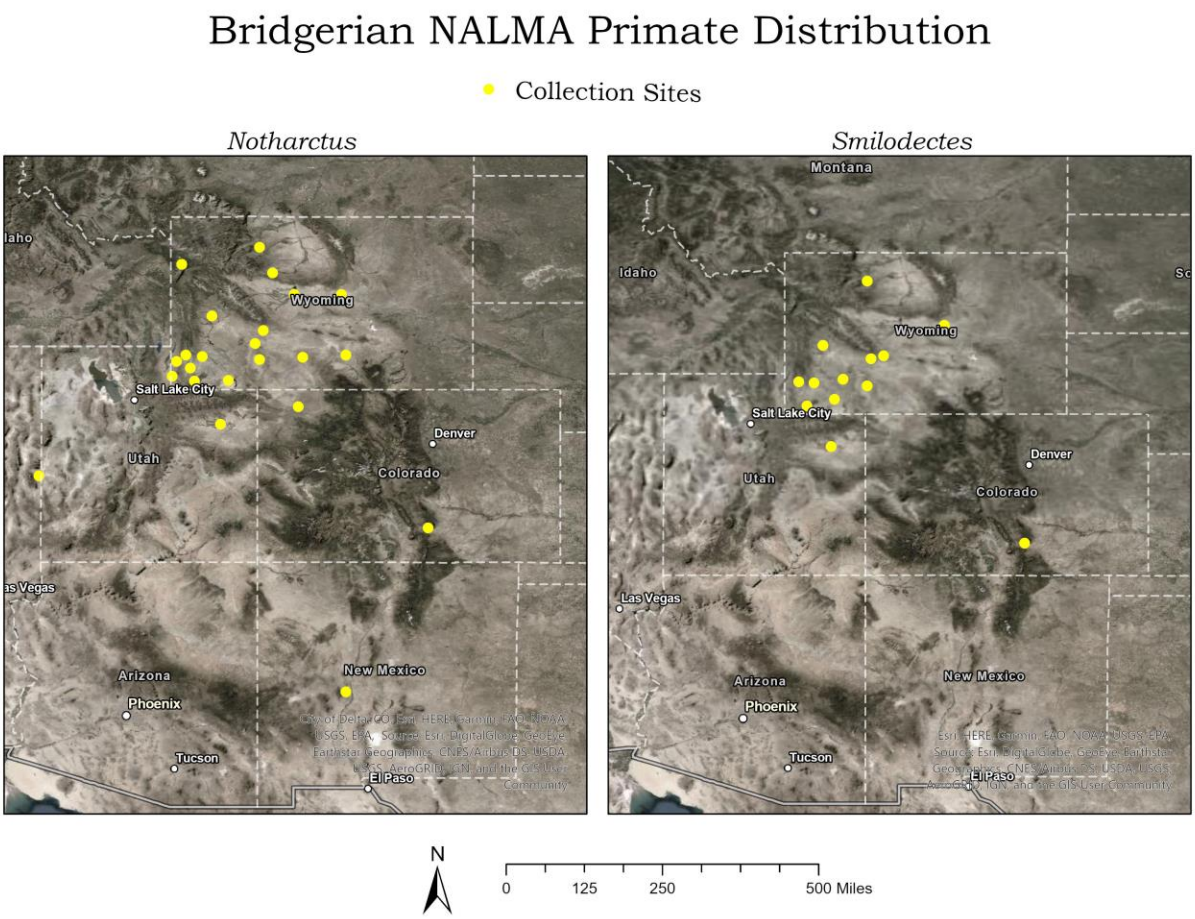

Figure 2. Geographic distribution of the Bridgerian Notharctine primates based on the location of collection sites. Collection Sites: Paleobiology Database (https://paleobiodb.org/#/).

Primate dental adaptations

To date, most of the research surrounding the Notharctine primates has analyzed the dental remains, and this project builds upon this tradition. Teeth are among the most abundant vertebrate fossils recovered in the fossil record due to their mineralization, hardness, and compact size (Fleagle, 2013). Paleoprimatologists have historically focused on the teeth because they can provide the baseline data required to develop a better understanding of primate evolutionary adaptations and behavior. Thus, teeth can provide critical insights into models of primate evolution since the dental morphologies that we

observe are considered to be adaptive responses to selective environmental factors and primate dietary patterns (Kay, 1975; Ungar, 1998; Cuozzo et al., 2012). Among the Order Primates, it has been suggested that the development of the alternating V-shaped crests and the triangular position of the molar cusps represents a basic molar morphology (Kay 1984). This dental morphology is suited for the shearing fibrous foods and crushing soft or hard foods (Kay, 1984). The morphology of primate dentition changes across time and space reacting to environmental selective forces and to the dietary regimes of primate species, and today we observe a great spectrum of variation across the Order Primates (Berthaume et al., 2020). The size of molars changes as well. In general, molar size and body size have an allometric relationship, and primate molar sizes can be used to estimate primate body mass (Kay, 1975).

Primate molars

Among primates, there are three major cusps on the upper molars: the paracone, the protocone, and the metacone (Figure 3). These three cusps form what is known as the trigon (Fleagle, 2013). Many primates, including *Cantius*, possess a fourth cusp known as the hypocone. The lower molars have three major cusps as well: the paraconid, the protoconid, and the metaconid. The cusps on the lower molars form the trigonid. Towards the distal end of the molars, an area referred to as the talanoid is formed by two or three other cusps. The two primary cusps that form the talanoid are the hypoconid and the entoconid, and some primates have developed a third cusps called the hypoconulid. The hypoconulid forms between the hypoconid and the entoconid and is positioned slightly distal to these cusps. A

close examination of the cusps of the teeth can uncover the history of primate evolution, which is the primary objective of this project (Fleagle, 2013).

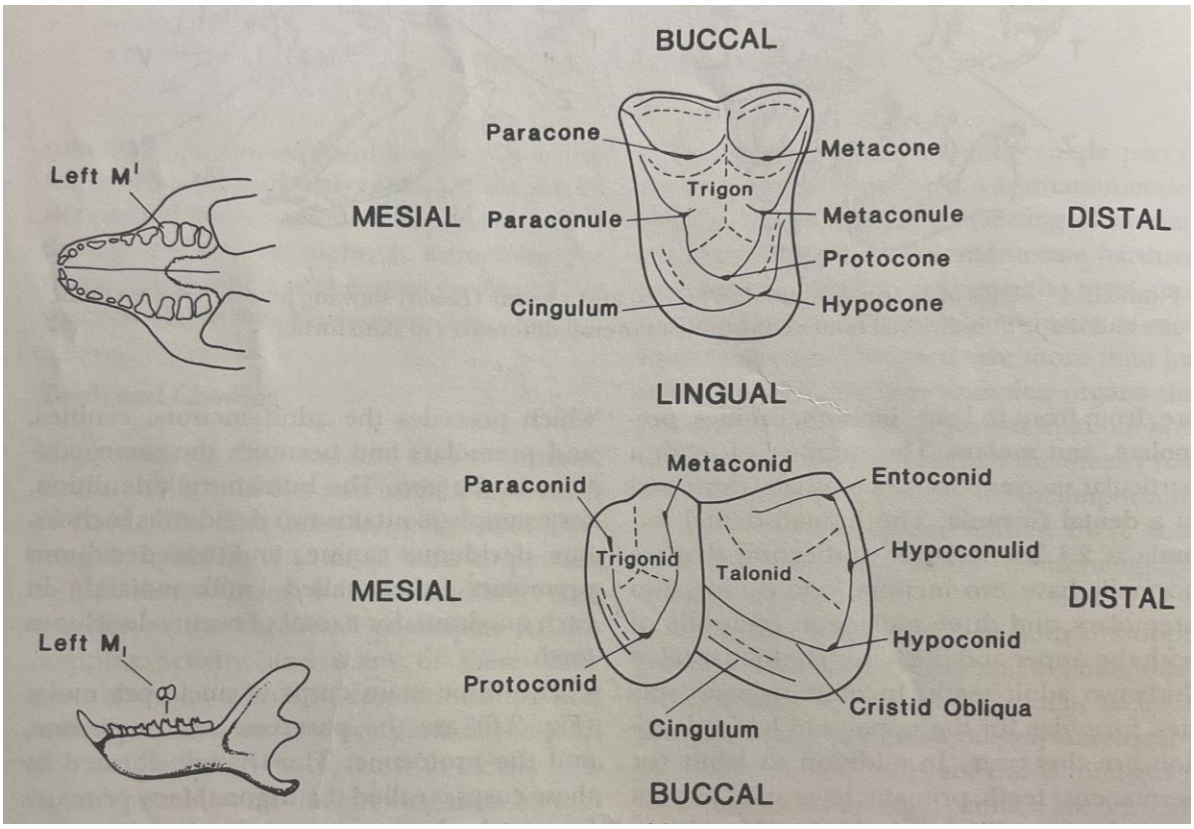

Figure 3. Illustration of primate molar morphology (Fleagle, 2013

Chapter 2

Background and Predictions

Climatic conditions in North America during the Eocene

Towards the end of the Paleocene, and throughout the entire Eocene Epoch (~55-41 mya), the earth experienced a period of global warming. Average Eocene temperatures were much warmer than the temperatures of the Paleocene, roughly 9 to 23°C higher. This period is divided into three climatic episodes, the Paleocene-Eocene Thermal Maximum, the early Eocene Climatic Optimum, and the Bridgerian Crash (Hyland et. al., 2013; Woodbourne, et. al., 2009). The period of global warming that occurred during the Eocene encouraged the immigration of several different mammalian groups into North America, including primates. Primates, along with artiodactyls and perissodactyls most commonly, appear in North America shortly after the Paleocene-Eocene Thermal Maximum. Specifically, the first appearance of primates occurs in the biostratigraphic zone known as the Wasatchian North American Land Mammal Age (NALMA) (Wa-0 to Wa-7), as noted above, these primates are known as the Notharctine primates (Beard, 2008; Woodbourne, et. al., 2009).

The Eocene is characterized by three primary climatic episodes: the Paleocene-Eocene Thermal Maximum (PETM), the Early Eocene Climatic Optimum (EECO), and the Bridgerian Crash (BC). The PETM occurred on the Paleocene-Eocene boundary which also marks the beginning of the Wasatchian (Wa-0 to Wa-7) North American Land Mammal Age (NALMA), an important stage in the evolutionary history of North American primates. The EECO begins towards the conclusion of the Wasatchian NALMA, extending into the Bridgerian NALMA (Wa-6 to Br-1a). The Bridgerian Crash occurred in the later Bridgerian

(Br-1b to Ui-1) and into the early Uintan stages. Each stage is characterized by distinctive climate and faunal communities that are important to consider when studying the mammalian evolution that occurred throughout the duration of Eocene (Woodbourne et al., 2009).

The Paleocene-Eocene Thermal Maximum (PETM)(Wa-0) is characterized by an increase in the average land air temperatures of the northern hemisphere, ranging from 9 to 23°C higher than that of the late Paleocene (Figure 4). This rapid spike in temperatures can also be observed in average sea surface temperatures, with an increase of approximately 8 to 16°C higher than the average sea surface temperatures of the late Paleocene (Inglis, et. al., 2020). The combination of these data would suggest that North America had developed into a subtropical climate with the transition from the Paleocene to the Eocene (Inglis, et. al., 2020). To further support this model, paleobotanists have identified the transition from a dry climate to a subtropical climate by examining the plant remains that date back to the onset of the PETM (Gingerich, 2006). During the late Paleocene most of the vegetation in North America consisted of small-leaved plants that are found primarily in dry climates, however, after the onset of the PETM, the floral remains include plants that would only be supported by a much more tropical climate (Gingerich, 2006).

It appears the rapid climatic change during the PETM was closely related to the increase in mammalian diversity from this time, more so than the climatic modifications that took place during the Cenozoic Era, before the onset of the PETM. The Cenozoic Era is known as the “Age of Mammals,” due to large number of mammalian fauna that make their first and last appearances. However, the floral and faunal remains from the early Cenozoic do not provide as much evidence for increased diversity when compared to the evidence from the PETM (Gingerich, 2006; Woodbourne, et. al., 2009). The increase in mammalian diversity

have been attributed to levels of competition and predation which may better explain this process prior to the episode of global warming that occurred at the end of the Paleocene. However, this is not the case for the PETM as it appears that the climatic conditions played a direct role in the increase of diversity of late Paleocene and Eocene mammals (Gingerich, 2006).

The transition from the Paleocene to the Eocene marks the first appearance of most modern orders of mammals, including Primates, Artiodactyla, and Perissodactyla. These orders appeared suddenly in the fossil record with very little evidence of their dispersal into North America (Gingerich, 2006). The comparatively sudden appearance of these immigrated mammalian genera, these early mammals were given their own biostratigraphic position (Wa-0) due to the fact that several of these species were much smaller than their modern-day relatives. This apparent size difference seems to be linked to the sudden climatic changes that the earth was experiencing during the Paleocene-Eocene boundary, as the trend towards smaller body sizes seems to disappear as the Eocene continues (Gingerich, 2006). One method used to examine this process is to compare the body weights and tooth sizes of several different mammalian species. Morphological studies of mammals across evolutionary timescales have demonstrated that both body weight and tooth size did increase over time within several different mammalian species and lineages. This includes the genus *Cantius*, which throughout the Eocene changed in size which appears to be an evolutionary adaptation linked to the amount of vegetation available to the species during the immediate transition from the Paleocene to the Eocene (Gingerich, 2003; Woodbourne, et al., 2009).

After the PETM, the number of mammalian first appearances plateaued as a response to environmental stability. After the onset of the PETM, nine new mammalian genera

immigrated to North America, bringing the total number of genera to 72 during the early Wasatchian (Wa-0). This rapid increase was followed by subsequent increase of 13 genera, resulting in 95 genera, including three of the Notharctine primates: *Cantius*, *Pelycodus*, and *Copelemur* (Wa-1 and Wa-2) (Covert, 1990). After the PETM, from Wa-2 to Wa-4 there appears to be a decrease in the total number of mammalian genera from 95 to 89 (Woodboune, et. al., 2009). The decrease in genera has been attributed to the smaller amount of diversity exhibited within the Eocene mammals due to the rising aridity in North America. However, mammalian diversity begins to increase once again with the onset of the Early Eocene Climatic Optimum (EECO) (Woodbourne, et. al., 2009).

The EECO is characterized by yet another rapid increase in average temperatures and is characterized as the warmest period of the Cenozoic Era (Figure 4; Inglis, et. al., 2020). The increase in average temperatures ranged from 9 to 17°C higher than the average temperatures during the late PETM (Hyland, et. al., 2013). With this rapid increase in temperatures, the EECO also experienced an increase in the total amount of precipitation, with an approximate increase of 500 millimeters (mm) of annual rainfall. This increase in annual precipitation resulted in the diversification of vegetation resulting in environmental changes for the mammals inhabiting North America (Inglis, et. al.,2020). Further evidence of the transition from primarily folivores (i.e., leaf eating animals) to the presence of more frugivores (i.e, fruit eating animals), aligns closely with approximate dates of the onset of the EECO, which further suggests that there was an increase in diversity among all biota during the EECO, including a diversity in flora species (Gingerich, 2003). For example, during the late middle Wasatchian (between Wa-6 and Wa-7), the total number of mammalian genera increases to 98 (Figure 4), including the two other primary Notharctine primate genera: *Notharctus* and

Smilodectes (Covert,1990). The increase in genera during the Wasatchian is then followed by another increase, bringing the total number of mammalian genera up to 104 during the early Bridgerian (Br-1a) (Woodbourne, et. al., 2009).

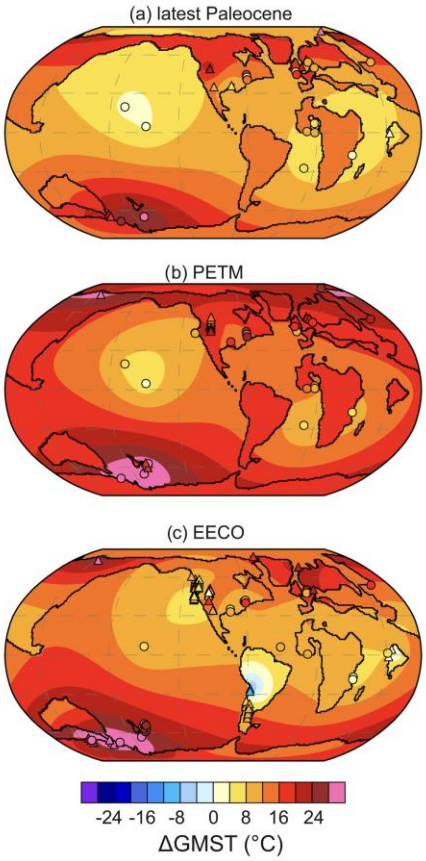

Figure 4. Temperature Changes during the PETM and EECO (Inglis, et. al., 2020).

The EECO, while incredibly important, was comparatively a short time period when viewed from a geological perspective only lasting about two million years (52 to 50 mya). However, during this time frame, the climate was changing rapidly. In addition, most of the Eocene mammalian fossil sites in North America support the supposition for rapid periods of change (Inglis, et. al., 2020). This can be demonstrated by comparing the periods of maximum mammalian diversity at each site with the periods in which the climate in North

America reached peak tropical conditions. In most cases, these two variables align. However, there is one site in western North America that would suggest otherwise. The Wind River Basin in Wyoming provides evidence of peak diversification occurring slightly later on the geological timescale as compared to the other sites in North America, implying that the climate must have been slightly different in the Wind River Basin (Hyland, et. al., 2013). This would suggest that this particular site could have reached a level of elevation high enough to create a type of site specific climate control, which in turn would encourage a different reaction to the rapid climate change occurring during the EECO as compared to the other fossil sites (Hyland, et. al., 2013).

By the end of the EECO (Br-1a), the overall diversity of mammalian genera was reduced by 19% (Woodbourne, et. al., 2009). This massive reduction in diversity is known as the Bridgerian Crash (BC)(Br-1b-Br-3). During the Bridgerian Crash the number of mammalian first appearances dropped precipitously, while the number of last appearances gradually increased (Figure 5). The Bridgerian Crash is characterized by a transition to a much cooler and arid climate, similar to the climate of modern-day western North America. Therefore, the evidence of fluctuating diversification during this time further supports the hypothesis that North American mammalian evolution in the Eocene was directly impacted by the dynamic changes in the climate (Woodbourne, et. al., 2009).

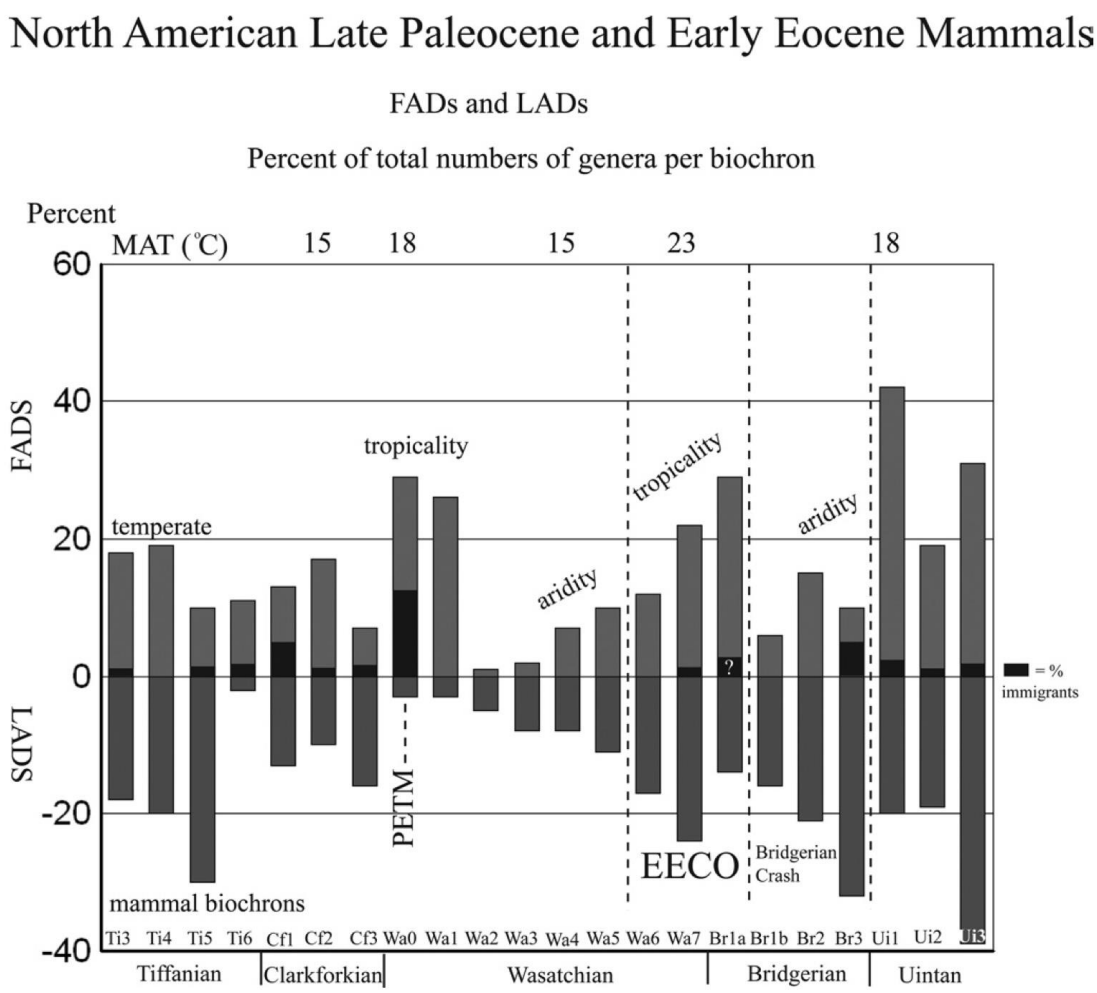

Figure 5. Representation of the First and Last Genera Appearances (MAT: Mean Annual Temperatures; FADs: first appearance of datum; LADs: last appearance of datum) (Woodbourne, et. al., 2009).

The Importance of the Genus *Cantius*

The first genus of the Notharctine primates to appear was *Cantius*, which consisted of six to ten species. However, the identification of the species in the genus have been historically difficult. For example, some *Cantius* species, including *C. ralstoni*, *C. mckennai*, *C. abditus*, and *C. frugivorous*, were identified as *Pelycodus*, a related genus that appears in the North American fossil record (Beard, 1988; Gingerich and Haskin, 1981). After further analysis, it was suggested that the primitive dental morphology of the earliest species of what was then

"*Pelycodus"* were different from that of the later *Pelycodus* specimens, which was one of the deciding factors in the transfer of the early "*Pelycodus*" specimens to the genus *Cantius*. Since the identification of this genus, *Cantius* has been recognized as the stem genus for the Notharctine primates based on the suggestion that the Notharctine primates reached North America by way of Europe during the influx of mammalian genera into North America after the onset of the PETM (Gingerich and Haskin, 1981; Inglis, et. al., 2020).

Cantius was a medium sized primate with an average body weight of about 3 kilograms (kg). However, the early species were considerably smaller with an average weight of about 1 kg (Gingerich, Smith, and Rosenberg, 1982). The increase in size may be attributed to the increase of available vegetative biomass resulting from warmer temperatures. The dental microstructure and molar morphology of *Cantius* suggest that this genus was primarily frugivorous (Mass and O'Leary, 1996) and in increase in available fruit biomass may have resulted in the larger body sizes of the genus. The post cranial morphology of *Cantius* is similar to modern-day arboreal primates with adaptations for vertical clinging and leaping including powerful grasping digits (Gebo, Dagosto, and Rose, 1991; Rose and Walker, 1995).

The dental and gnathic traits of *Cantius* provides for the most robust comparisons to extant and extinct primates. *Cantius* possessed an unfused mandibular symphysis, a trait commonly observed in most omomyids. However, *Cantius* has been identified as an adapid primate (Beard, 1988). The presence of an unfused mandibular symphysis is only observed in the early adapid genera, which places *Cantius* into a transitional position between omomyids and adapids (Fleagle, 2013). Given that the mandibular morphology of *Cantius* suggests that it is an early transitional group of primates, the genera itself underwent a series of gradual

changes as the Eocene proceeded (Beard, 1988; Covert, 1990). One approach to tracking the changes of within the genus is through the study of the most prominent elements discovered, the molars.

The lower molars of the genus *Cantius* are characterized by the appearance of five major cusps: the paraconid, protoconid, metaconid, hypoconid, and the entoconid. The position of the paraconid, protoconid, and the metaconid result in the mesially positioned trigonid, while the hypoconid and entoconid create the distally positioned talonid (Beard, 1988; Covert, 1990). The molars are relatively broad, with the second molar appearing to be almost square in shape. On the M_1, the paraconid is placed mesiolingually towards the corner of the molar, while the paraconid on M_2 is closer to the metaconid towards the distal end of the molar. As for the M_3, the tooth is much longer with evidence of a hypoconulid, the distal most fifth cusp that is located between and directly behind the hypoconid and entoconid (Covert, 1990).

The upper molars are different considering that these molars consist of only three cusps: the paracone, protocone, and metacone. These three cusps make up the trigon on the upper molars, and create a conical-like, almost triangular, shape that it observed throughout all of the species of *Cantius*. The upper molars show evidence of an extreme Nannopithex-fold, rather than a fourth cusp. However, as time passed, the later species exhibited a prominent Nannopithex-fold that is commonly referred to as a "pseudohypocone" (Covert, 1990). The term pseudohypocone is given since this feature is difficult to identify as an actual cusp. However, in terms of the Notharctine primates, the pseudohypocone should be considered an actual hypocone, as with time this trait became more prominent (Anemone, Skinner, and Dirks, 2012).

The dental morphology of the genus *Cantius* is important to understand because *Cantius* is considered the stem genus for the Notharctine primates. Many of the dental morphological traits observed in *Cantius* are found among the remaining Notharctine primates (Table 1). There are three primary hypotheses regarding the origin of the Notharctine primates, each linked to *Cantius*. The first hypothesis suggests that the Notharctine primates are monophyletic in origin, resulting in a direct line from *Cantius*. The second hypothesis suggests Notharctine primates are polyphyletic in origin with the later genera evolving from both *Cantius* and *Copelemur* (Beard, 1988; Gingerich and Simons 1977). The third hypothesis suggest that the Notharctine primates may be paraphyletic in origin, suggesting that this group of primates evolved from the genus *Cantius*. However, a paraphyletic origin may be unlikely given that each Notharctine genera would have evolved from different species of *Cantius*. For example, *Copelemur* has similar dental morphology when compared to the younger *Cantius* species (e.g., *C. frugivorous*) while *Pelycodus* is more similar to the older *Cantius* species (e.g., *C. torresi*) (Gunnell, 2002).

The genus *Cantius* is also important to primatologists because it has been considered ancestral to the Malagasy lemurs. Notharctine primates are often referred to as the first "lemur-like" primates to emerge (Beard, 1988, Covert, 1990). The relationship between the Notharctine primates and lemurs are predicated largely on similar dental morphologies, including the overall shape of their teeth. The upper molars of Malagasy lemurs exhibit the three-cusp morphology, resulting in a tribosphenic shape. The size of the some Notharctine primate molars is also very similar to the size of some species of extant Malagasy lemurs.

Summary of the diagnostic traits of each Notharctine genera

Table 1 presents each of the Notharctine genera, their stratigraphic appearance (Figure 6), and the diagnostic dental morphological traits associated with each genus.

Table 1. Summary of dental morphological traits associated with each Notharctine genera.

Genus	Stratigraphic Appearance	Upper Molars	Lower Molars
Cantius	Wa0 – Br1a	Three cusps (paracone, metacone, and protcone), Nannopithex-fold that develops into a pseudohypcone, small metaconule and protoconule, cresitform mesostyle.	Five cusps (paraconid, metaconid, protoconid, hypoconid, entoconid, and hypoconulid), mesially positioned trigonid, elongated talonid.
Copelemur	Wa4 – Wa7	Three cusps (metacone, paracone, and protocone), Nannopithex-fold, strong mesostyle, and a weak metaconule.	Six cusps (paraconid, metaconid, protoconid, hypoconid, entoconid, and hypoconulid), presence of entoconid notches on the molars, anteriorly shifted paraconid.
Pelycodus	Wa6	Four cusps, signature trigon with the development of a distinct hypocone on the first and second molar, small paraconule, lacking a metaconule, lacking a mesostyle.	Four cusps, lacking a paraconid and hypoconulid, lacking entoconid notches, small paraconid and protoconid.
Notharctus	Br0 – Br2	Four cusps, signature trigon with a distinct hypocone, well-developed mesostyle,	Six cusps, trigon and talonid with a distinct hypoconulid, narrow molars, reduced paraconid,

		rectangular shaped third molar.	presence of the entoconid notches.
Smilodectes	Br1a – Br2	Four cusps, signature trigon with a small diminutive hypocone and well developed protocone, mesially positioned paracone, large metaconule, crestiform mesostyle	Five cusps, lacking a paraconid with a weak entoconid, narrow molars, presence of entoconid notches.

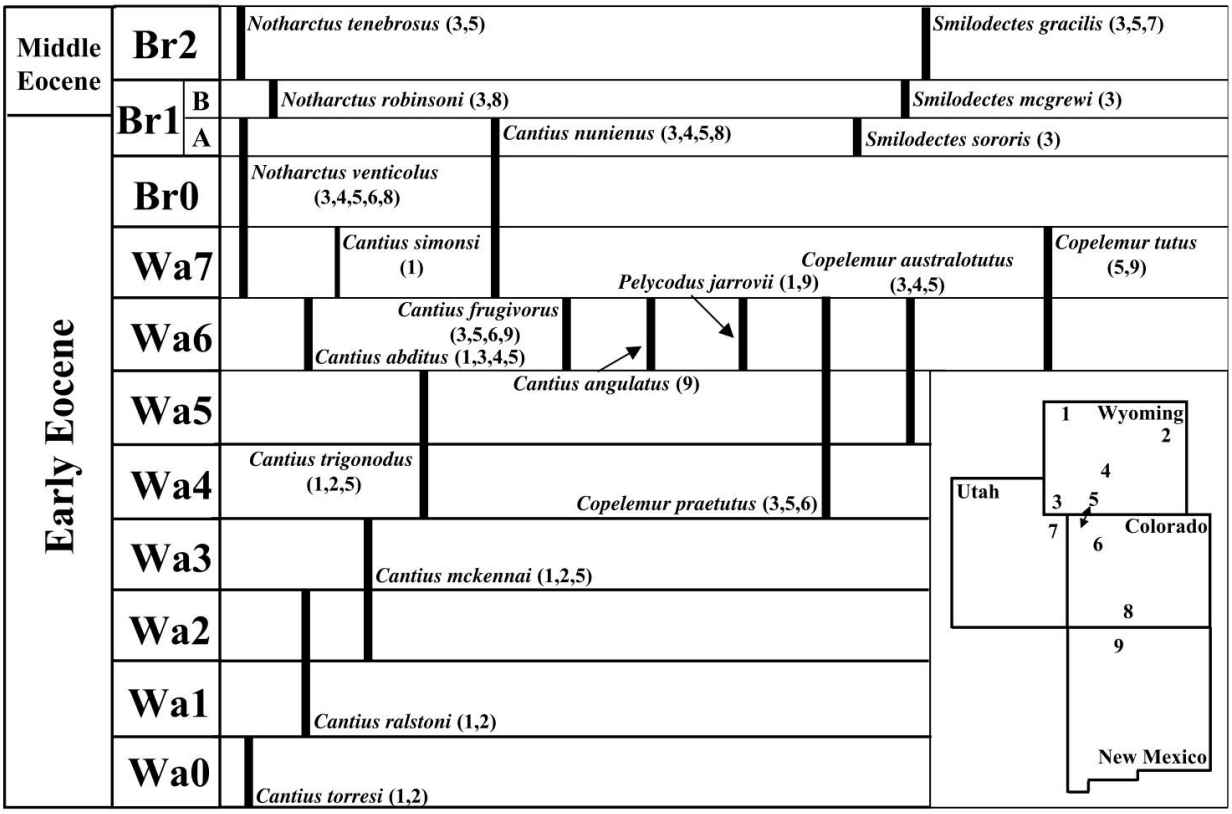

Figure 6. Stratigraphic distribution of the Notharctine primates across Colorado, New Mexico, Utah, and Wyoming (Gunnell, 2002).

The benefits of digital restoration

The specimens for this project were scanned using a micro computed tomography (CT) scanner and then analyzed using images generated by Avizo, a three-dimensional reconstruction software. This allowed for further morphological analysis of the dentition.

This approach improves our understanding of the taxonomy *Cantius* given that most of specimens of the genus are teeth. The dental morphological traits examined in this project are difficult to analyze with the human eye and without the aid of instruments (i.e., microscope or stereoscopes). Creating three-dimensional reconstructions of these teeth allows for comparisons of specimens within the same genus, same locality, and among different primate species.

Using CT scans is becoming a more common practice and is being used more frequently by researchers to digitally preserve, analyze, and reconstruct fossils (Cunningham, et. al., 2014). This is an important practice given that even under the very best conservation conditions, fossils are incredibly fragile and often break during handling and examination. Fossils have also been lost and subsequently are no longer available to study by the scientific community (Cunningham, et. al., 2014).

Scanning fossils using a micro CT scanner is a non-invasive technique that does not damage the specimen itself. This is especially important for specimens that are extremely rare or are historically important. Digital approaches to studying and storing the morphologies of extant and extinct species has recently be referred to as "Virtual Anthropology" (Weber, 2015). Three-dimensional images of skeletal and dental elements can be uploaded into 3D databases that act as virtual repositories. These images can be downloaded and printed using a 3D printer, available to anyone across the globe. For teaching purposes, 3D printed casts can be used by professors and students in traditional and virtual classrooms to help visualize the fossils and understand their evolutionary relationships to other species (Cunningham, et. al., 2014; Uldin, 2017). For example, a 3D scan of the hominin skull of *Homo naledi* was recently uploaded to MorphoSource

(https://www.morphosource.org/), a popular digital repository for biological specimens. Biological anthropology instructors have printed casts of the *H. naledi* skull and incorporated these casts into their teaching curricula.

The three-dimensional images generated from this study will ultimately be uploaded to a digital repository. There the images will be available to the online community. This will enable researchers to examine the specimens with great detail online and generate their own casts using a 3D printer. Casts generated from this study will be useful for both scientific inquiries and for the purposes of pedagogy.

Predictions

This study is largely descriptive, however, the methods used in this study allow for the generation of two predictions that will be examined throughout this project.

Prediction 1: Given that the taxonomy of the mammals from Tim's Confession, the locality in which the specimens for this project were recovered, has been well described and examined, I predict that the dental morphological data from this thesis will support the existing classification of these specimens.

Prediction 2: Previous research suggests that the genus *Cantius* may possibly be ancestral to extant Malagasy lemurs given the fact that this genus exhibits lemur-like morphologies. I expect that the dental morphology of the *Cantius* specimens examined in this study should be similar to extant lemurs of the same size and dietary pattern. This would include the overall shape, size, and cusp patterns.

Chapter 3

Materials and Methods

This project utilized two broad approaches to identify the alpha taxonomy of the *Cantius.* The first approach is a qualitative analysis consisting of the images generated by Avizo. The second approach is quantitative analysis of the measurements of the molars of these specimens, along with the measurements of 103 other *Cantius* specimens.

Shared Materials and Instrumentation Facility

For this project, ten specimens belonging to the genus *Cantius* and one specimen of the genus *Copelemur*, were examined. Fossil specimens were scanned using a micro computed tomography (CT) scanner located at the Shared Material and Instrumentation Facility (SMIF) at Duke University. Each specimen scanned is a part of the permanent collection at the Carnegie Museum of Natural History in Pittsburgh, Pennsylvania. Most of the specimens were collected from Tim's Confession, a productive mammalian fossil locality found in the Great Divide Basin of Wyoming. Tim's Confession has been identified as Carnegie Museum Locality 4026.

Tim's Confession dates to the early Eocene, specifically Wa4. The dates of Tim's Confession have been identified based on the discovery of *Tetonius matthewi*, an omomyid dated to the same biozone (Bown and Rose, 1987). Three of the specimens included in this study (CM 93347, CM 93349, CM 95509) were collected from different sites. CM 93347 was collected from Hill 7125, Carnegie Museum Locality 168. CM 93349 was collected from North Hill 7185, Carnegie Museum Locality 176. Finally, CM 95509 was collected from Scorpio, Carnegie Museum Locality 154. All the specimens were collected by field

crews under the instruction of Dr. Robert L. Anemone from the University of North Carolina at Greensboro (Table 2). The specimens that were selected for this project were chosen based on the fact that the teeth were still set inside of the mandibular or maxillary fragments which in turn makes it easier to identify the position of the tooth for a more accurate analysis. Most of the specimens selected also include multiple teeth, except for two of the specimens, CM 95510, and CM 95512, that contain only a single tooth.

Table 2. List of specimens selected for scanning including the Carnegie Museum number for each specimen, primate genus, and fossil element(s).

Carnegie Museum #	Taxon	Element(s)
93347	*C. frugivorous*	Right Maxilla. M1-M3
93349	*C. frugivorous*	Left Mandible. P4-M2
95509	*Copelemur australotutus*	Left Mandible. P3-M1
95510	*C. trigonodus*	Right Mandible. M2
95511	*C. ?*	Left Mandible. M2-M3
95512	*C. ?*	Right Mandible. M3
95513	*C. ?*	Left Maxilla. P3-M3
95514	*C. ?*	Right Mandible. P4-M1
95515	*C. ?*	Right Mandible. M1-M2
95516	*C. trigonodus*	Right Mandible. P3-M3
95517	*C. trigonodus*	Right Maxilla. M2-M3

The micro CT scanner located at SMIF is a Nikon XTH 225 ST scanner with a Perkin Elmer 1620 AN3 X-ray detector panel (Shared Materials and Instrumentation Facility). The

specimens were packaged in plastic containers imbedded in packaging foam to secure the fossils in place. The specimens were then placed onto a rotating metal platform inside of the micro CT scanner and adjusted to the appropriate position for the scans to remain in the frame for the duration of the rotation. The CT scanner obtains radiographs, or projections, of the fossils from multiple different angles to generate the best overall reconstruction of the specimen (Cunningham, et. al., 2014). Due to the larger number of projections required to accurately reconstruct these specific specimens, the scanning duration ranged from 30 to 60 minutes. Scanning duration varies for each specimen due to several factors including the time required for the CT scanner to warm-up if needed, the number of projections required for the best reconstruction of the specimen that was analyzed, the exposure time, the honing of the platform inside the CT scanner, and the time required for the X-rays to reach optimum conditions.

Once the scanning of the specimens was completed, the images were imported directly from the CT scanner to the reconstruction computers, RECO1 and RECO2, and reconstructed TIFF stacks were created for further analysis. The reconstructed TIFF stacks were then imported into Avizo Lite, a three-dimensional visualization software downloaded onto RECO3, the computer used for the post processing of CT data. After the reconstructed TIFF stacks were imported into Avizo, the crop editor tool was used to invert the data into its' proper orientation. Before further analysis, the option to smooth and restore the surfaces of the fossils is available if this is needed for the specimen being analyzed. This process is done by using the segmentation option in Avizo to fill these holes and cracks is available by choosing the "fill holes" option (Lautenschlager, 2016). The colormap was then chosen. The next step incorporated Volume Rendering (Figure 7), as this process recreates the casting of

light rays. This function allows for the highlighting of specific features on the fossils, for the images in this project, the “specular” lighting option was applied. The “specular” lighting highlights the peaks of the teeth, which can be beneficial when working with teeth that are worn. After using the Volume Rendering function to adjust the reconstruction to the appropriate settings, the next step was to set the reconstruction in the preferred position. For this project, the primary area of focus is the occlusal surface of the teeth because the cusps of the teeth provide the data needed to understand the taxonomic placement of these primates. Specimens that included the alveolar bone are depicted showing the lateral surface as well.

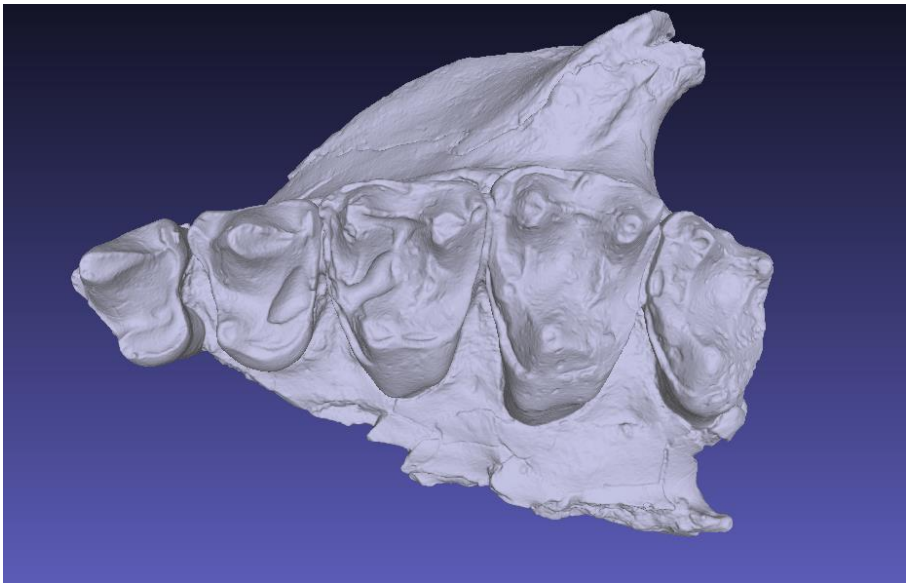

Figure 7. Example of a 3D visualization of CM 95513, a *Cantius trigonodus* specimen including the P^3 – M^3, created in Avizo provided by Dr. Robert Anemone.

Cantius molar measurements

In addition to scanning the eleven specimens using the micro CT scanner, 103 *Cantius* molars were measured using digital calipers for comparison (See Appendix). The specimens measured were primarily collected from Tim's Confession. In addition, some of the specimens were collected from another fossil locality known as North Hill. This project primarily examines the upper and lower molars given that there were very few premolars for comparison. In total this study measured 32 upper molars consisting of two M^1 specimens, 13 M^3 specimens, and 17 unidentified upper molars. As for lower molars, 71 molars were measured consisting of 19 M_1 specimens, 32 M_2 specimens, 19 M_3 specimens, and one unknown lower molar. Although the dataset of measured molars is rather large, most specimens belonged to *C. trigonodus*, collected from one locality. The nature of these data unfortunately precludes robust statistical comparisons. However, basic measures of central tendency and variation were calculated.

Chapter 4

Results

The results of this study are presented in three sections. The first includes a description of each Avizo reconstruction for each specimen. Second, a brief summary of each of the specimens' classification based on the dental morphology provided by the Avizo reconstructions. Finally, the chapter concludes with an analysis of the molar measurements of the teeth examined in this study.

Avizo reconstructions

CM 93347

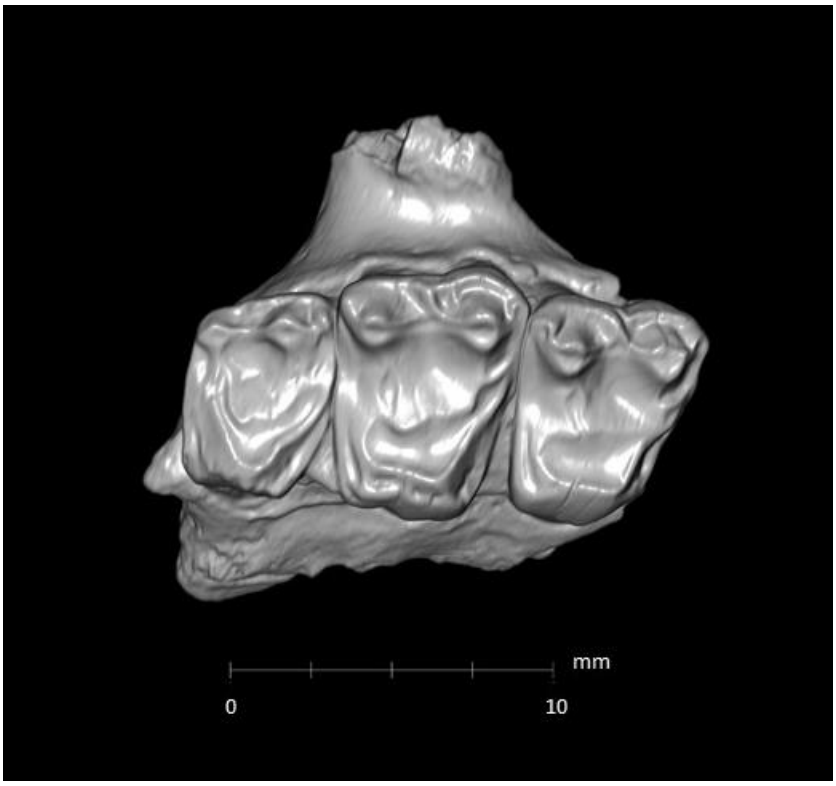

Figure 8. Occlusal Surface of CM 93347, a *C. frugivorous* specimen with M^1-M^3. Mesial to the right of the page; buccal to the top of the page.

CM 93347 (Figure 8) has been identified as a right maxilla containing all three molars, M^1-M^3. All three molars have distinct paracones and metacones, with a much less pronounced protocone. The hypocone has not yet formed for this specimen, however, there appears to be a well-developed Nannopithex fold, or postprotocingulum located posteriorly to the protocone. The buccal cingulum appears to become more distinct between the paracone and the metacone on M^1 and M^2 as if a mesostyle is to take formation, and it appears as though a slight mesostyle has begun to form on M^2 buccal to the paracone and metacone. However, M^1 does not appear to have an actual mesostyle, but still has rather strong buccal cingulum. The mesiolingual cingulum and postcingulum are both pronounced but the two cingula do not meet to create a continuous crest around the lingual portion of the tooth.

CM 93347 has been previously identified as belonging to *Cantius frugivorous*, a species that appears towards the end of the early Eocene and is considered a younger species according to the geological time scale (Covert, 1990). Based on the dental characteristics visible in the reconstruction shown in Figure 8, there is evidence to suggest that this species could have been misidentified, but there also appears to be evidence to suggest that this does belong to *C. frugivorous*, making the identification of this species difficult to definitively classify. For example, the lack of a hypocone or pseudohypocone with the presence of a strong Nannopithex fold is commonly found in older species of *Cantius* (Beard, 1988; O'Leary, 2021). On the other hand, the presence of a slight mesostyle on M^2 would suggest that this specimen does belong to *C. frugivorous*, given the fact that developed mesostyles are uncommon in other *Cantius* species, including *C. torresi, C. ralstoni,* and *C. mckennai*.

After further consideration, the presence of the slight mesostyle on M^2 seems to be the more distinctive characteristic, which encouraged me to leave the species identification as is.

CM 93349

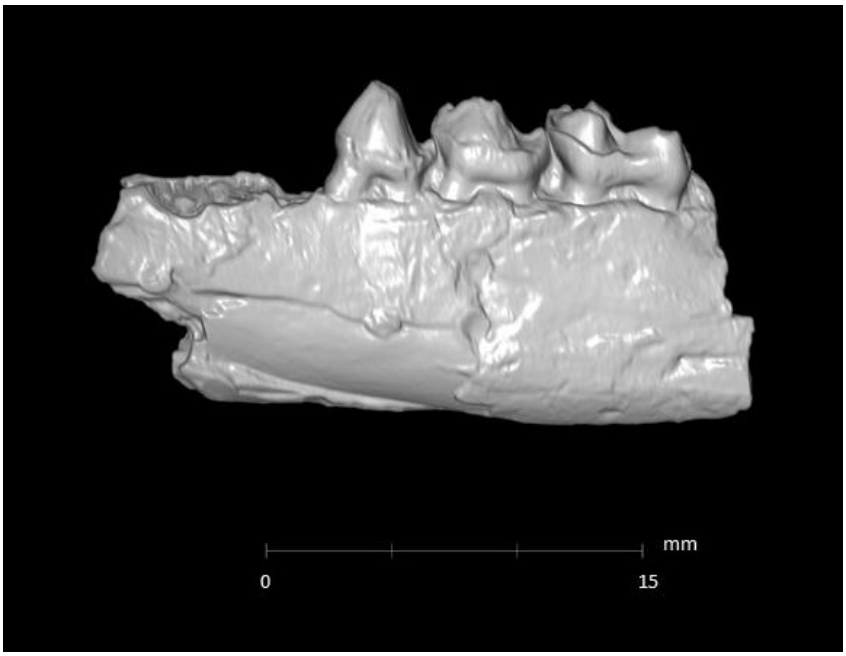

Figure 9. Lateral Surface of CM 93349, a *C. frugivorous* specimen with P_3-M_1. Mesial to the left of the page.

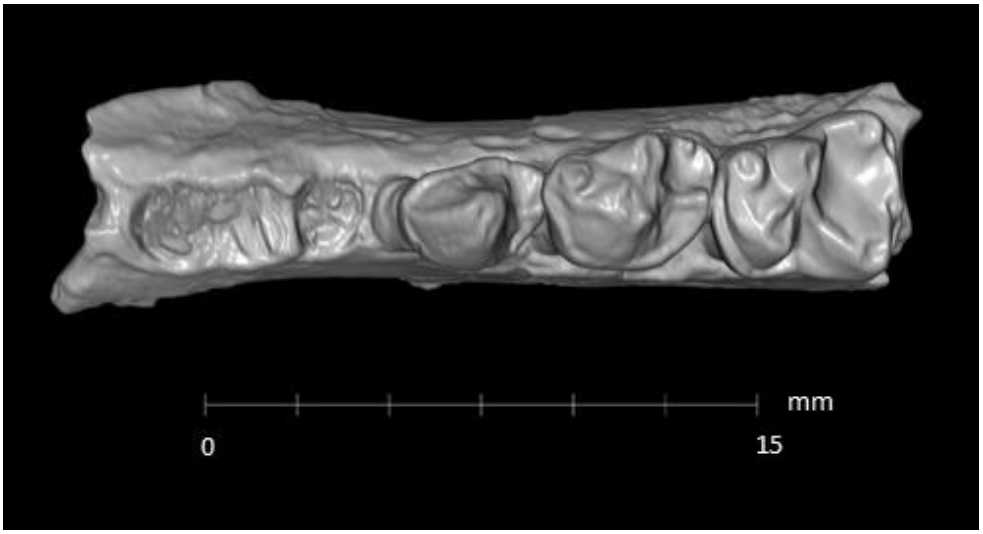

Figure 10. Occlusal Surface of CM 93349, a *C. frugivorous* specimen with P_3-M_1. Mesial to the left of the page; buccal to the bottom of the page.

CM 93349 has been identified as a left mandible containing a premolar and two molars, P_4-M_2. P_4 appears to have a less pronounced, if not absent, paraconid with a very distinctive protoconid that appears canine-like. Both molars, M_1 and M_2, have the distinctive trigonid including the paraconid, metaconid, and protoconid (Figure 10). The M_1 appears to have a rather robust protoconid. The paraconid and metaconid are also positioned further apart on M_1 as compared to M_2. It also appears as though the talonid, consisting of the hypoconid, entoconid, and hypoconulid, is similar in length mesiodistally to that of the trigonid on both the M_1 and M_2, however, it does seem to be slightly longer than the trigonid on the M_2. It is also clear that the M_2 has an entoconid notch, a trait found in very few *Cantius* specimens (Figure 9).

CM 93349 has been previously identified as *C. frugivorous*, similar to CM 93347. *C. frugivorous* is known to be a younger species, and the presence of the entoconid notch further suggests that this identification is indeed correct given the fact that entoconid notches are known to be found in the younger *Cantius* species (O'Leary, 2021). The robusticity of the trigonid cusps, and the longer talonid are also common characteristics observed in *C. frugivorous*. After reviewing the dental characteristics, I suggest that the initial identification of this specimen was correct, therefore, the species identification remains the same.

CM 95510

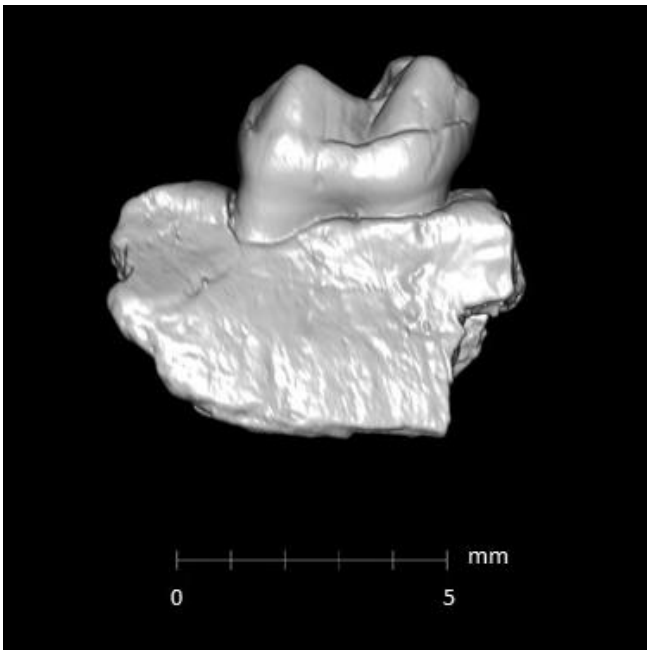

Figure 11. Lateral Surface of CM 95510, a *C. trigonodus* specimen with M_2. Mesial to the right of the page.

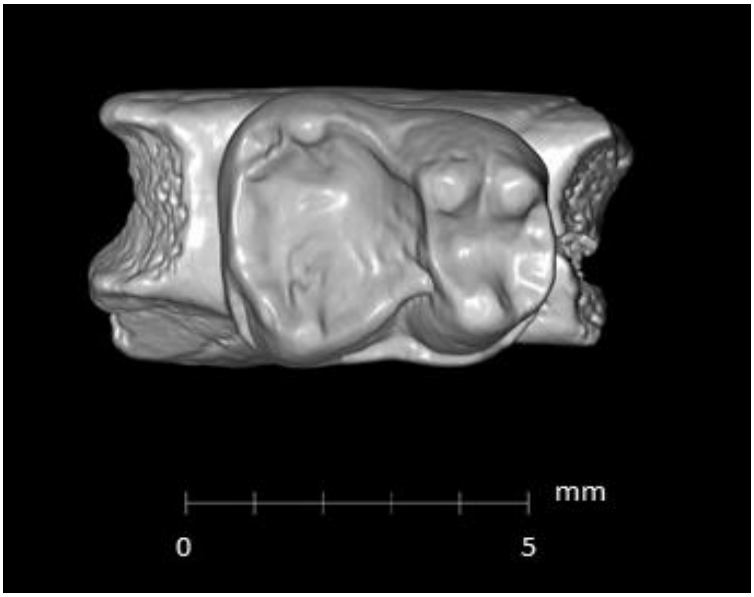

Figure 12. Occlusal Surface of CM 95510, a *C. trigonodus* specimen with M_2. Mesial to the right of the page; buccal to the bottom of the page.

CM 95510 has been identified as lower right M_2. The M_2 has the distinctive trigonid, observed in most primate species consisting of three very distinctive cusps, the paraconid, metaconid, and protoconid (Figure 12). The paraconid and metaconid are positioned close together, creating a very narrow trigonid. The talonid, including the hypoconid, entoconid, and less pronounced hypoconulid, is much longer mesiodistally as compared to the trigonid. CM 95510 appears to be lacking an entoconid notch, a feature that distinctively aids in the identification of the species (Figure 11). This specimen also appears to have adapted a larger overall molar size, with a length of 4.61 mm and a width of 3.99 mm.

CM 95510 has been previously identified as *C. trigonodus*. *C. trigonodus* was previously identified as *Pelycodus trigonodus*, and *C. trigonodus* also has very similar dental traits to *C. frugivorous* which makes the species identification for this specimen difficult to classify. Based on the data provided in the reconstruction (Figure 11) depicting the lateral surface of CM 95510, this specimen is lacking entoconid notches, a trait commonly found among younger *Cantius* specimens (O'Leary, 2021). CM 95510 also has a rather large molar size. The maximum length of the M_2 in the *Cantius* specimens was 4.76 mm and the maximum width was 3.99 mm, very close to the measurements of CM 95510. The final distinctive trait is the elongated talonid. After careful consideration, I have determined that this specimen has been identified correctly as *C. trigonodus.* The absence of the entoconid notch was the key to determining the evolutionary position of this specimen, given that entoconid notches are one of the distinctive traits of *C. frugivorous* (Beard, 1988; O'Leary, 2021).

CM 95511

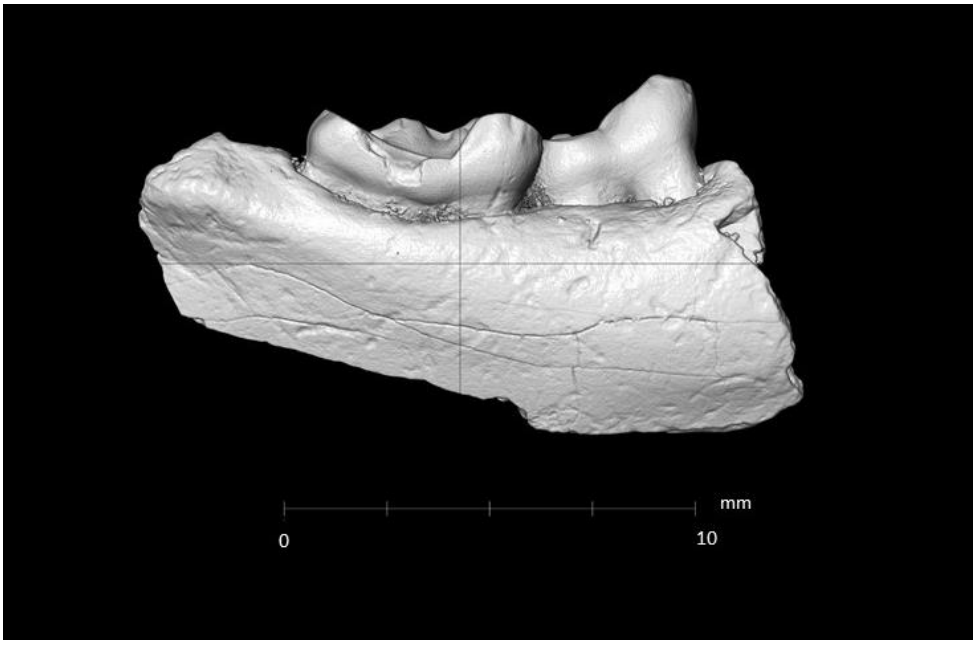

Figure 13. Lateral Surface of CM 95511, a *C. trigonodus* specimen with $M_2 – M_3$. Mesial to the right of the page.

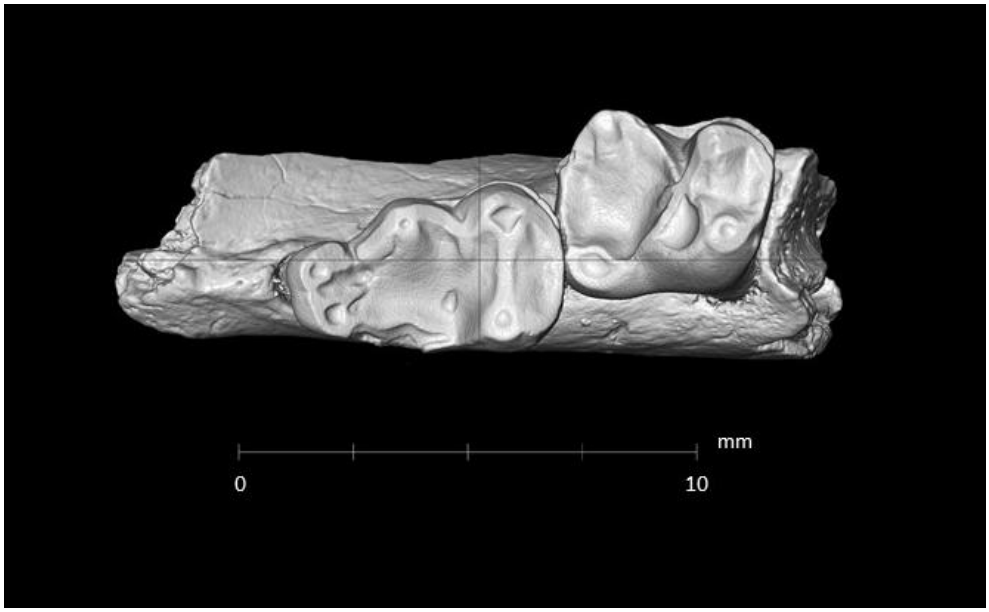

Figure 14. Occlusal Surface of CM 95511, *C. trigonodus* specimen with $M_2 – M_3$. Mesial to the right of the page; buccal to the bottom of the page.

CM 95511 has been identified as a left mandible, containing two molars, M_2 and M_3. The cusps on this specimen were difficult to determine due to the condition of the teeth. The teeth in this specimen show signs of extensive wear, especially the M_3. Multiple cusps have become pits, most likely due to the frugivorous diet of the genus *Cantius* (Beard, 1988; Covert 1990). Given the apparent misplacement of the M_2 on this specimen, this may have played a role in the wear on the M_3. The M_2 exhibits a distinctive trigonid, consisting of a closely positioned paraconid and metaconid, with the protoconid located buccally. The M_2 also appears to be comparatively shorter and wider. The talonid, consisting of hypoconid, entoconid, and weak hypoconulid, is mesiodistally longer than that of the trigonid, a trait commonly observed in *Cantius* specimens. CM 95511 also lacks entoconid notches, a characteristic observed in *C. frugivorous* (O'Leary, 2021).

To date, CM 95511 has been placed in the genus *Cantius* and has not been identified to the species level. The extensive wear on these molars made this specimen difficult to classify. However, after examining the reconstruction of the occlusal surface (Figure 14), there are a few distinctive characteristics that aid in the identification of this species, that being the elongated, rounded talonid and the overall size of the M_2, along with the known dates of the locality in which this was found. These characteristics lead me to suggest that this specimen can be identified as *C. trigonodus*.

CM 95512

Figure 15. Lateral Surface of CM 95512, a *C. trigonodus* specimen with M_3. Mesial to the right of the page.

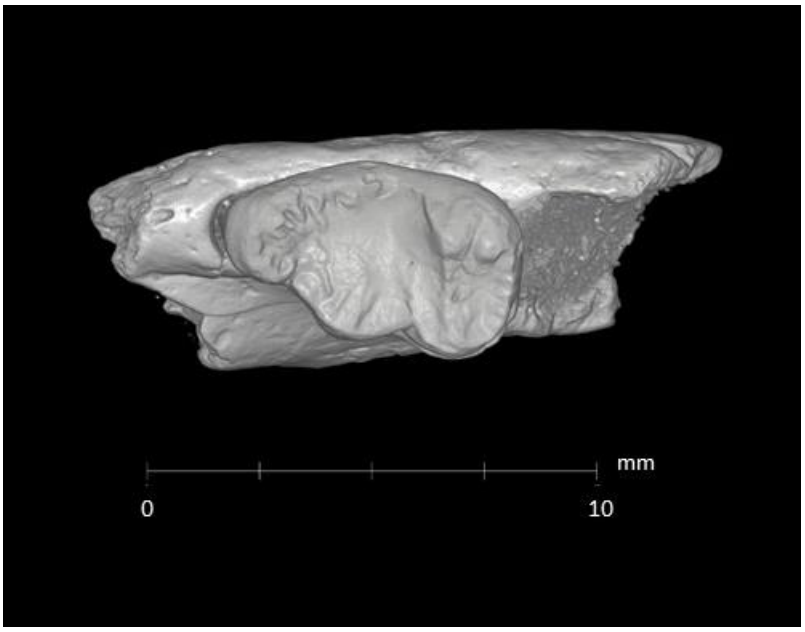

Figure 16. Occlusal Surface of CM 95512, a *C. trigonodus* specimen with M_3. Mesial to the right of the page; buccal to the bottom of the page.

CM 95512 has been identified as a right, lower third molar (M_3). The trigonid consists of the paraconid, a robust metaconid, and a weak protoconid. The trigonid is very small compared to the talonid, with the paraconid and metaconid positioned very close together. The cusps that create the talonid are difficult to identify when viewing the occlusal surface (Figure 16). However, the cusps are more visible from the lateral view (Figure 15). The hypoconid seems to be the most developed at the distal cusps, forming what appears to be a single, weak hypoconulid and a weak entoconid. The talonid is well-rounded, with evidence of extensive wear. The wear is similar to the pitting present in CM 95512, and the pitting was determined to have been a result of the frugivorous diet (Beard, 1988; Covert, 1990).

To date, CM 95512 has not been previously identified at the species level but placed into the genus *Cantius*. These reconstructions (Figure 15-16) have highlighted the dental morphological traits that will aid in the identification of the species. The dental characteristics include the closeness of the paraconid and metaconid which would suggest this is a shorter trigonid, the round talonid, and the single hypoconulid present on the distal end of the molar. These three distinctive traits are observed in individuals that have been identified as *Cantius trigonodus* (Covert, 1990). After reviewing the traits listed above, I suggest that this specimen can also be identified as *C. trigonodus*.

CM 95513

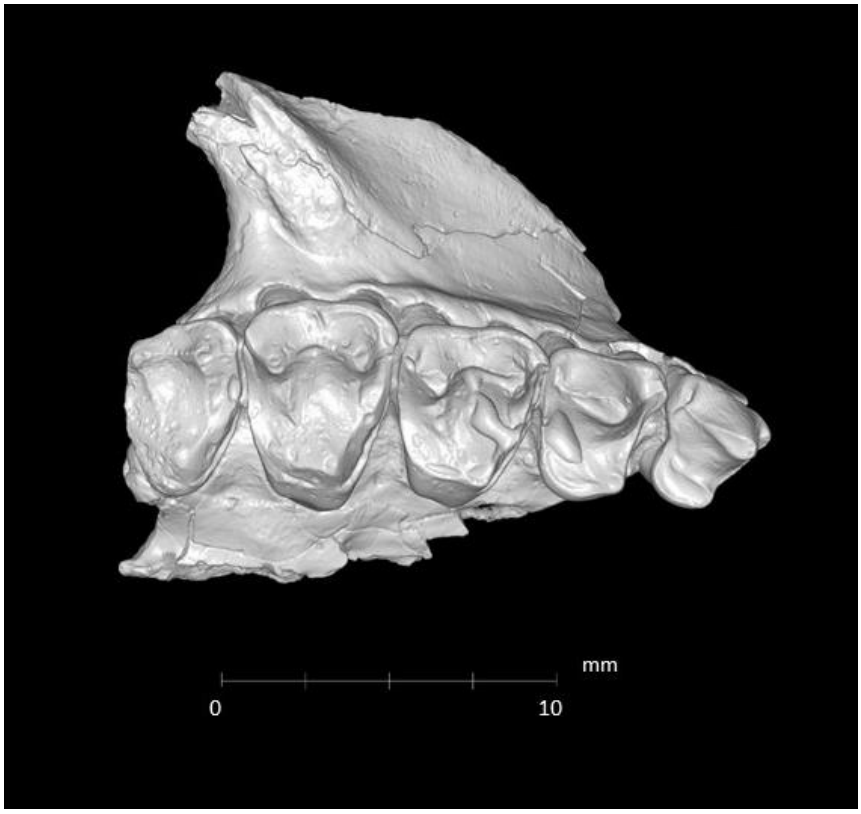

Figure 17. Occlusal Surface of CM 95513, a *C. trigonodus* specimen with P^3 – M^3. Mesial to the right of the page; buccal to the top of the page.

CM 95513 has been identified as part of a left maxilla including two premolars and three molars, P^3-M^3. The two premolars, P^3 and P^4, have rather robust paracones along with a weak protocone. The P^4 on this specimen is beginning to show early signs of molarization, a trait described in some lemur genera, most notably *Eulemur* (Gebo, 2014). The trigon on the molars, M^1-M^3, consist of well-developed paracones and metacones with a less developed protocone, however, the M^3 has a reduced metacone as compared to the metacones on the M^1 and M^2. The M^2 is rather broad buccolingually. There also appears to be a crestiform mesostyle between the paracone and metacone on the M^1 and M^2, however, the buccal cingulum is weak. The mesiolingual cingulum is very distinct but it does not connect to the

postcingulum. Due to the lack of connection, there is not a continuous crest around the molar. The M^1 and M^2 appear to have developed a strong Nannopithex-fold, but the M^3 appears to be lacking a Nannopithex-fold.

CM 95513 has not been previously identified at the species level. However, it has been placed into the genus *Cantius*, similar to the other specimens analyzed for this project. The reconstruction made here (Figure 17) aided in the identification of this specimen. The dental characteristics that were determinant in the identification process include the crestiform mesostyle, the presence of a strong Nannopithex-fold, and the size of the M^2 as compared to the other molars. These three specific traits are commonly found in individuals that have been identified as *C. trigonodus* (Covert, 1990). Based on this suite of traits, I suggest that CM 95513 can be identified as *C. trigonodus*.

CM 95514

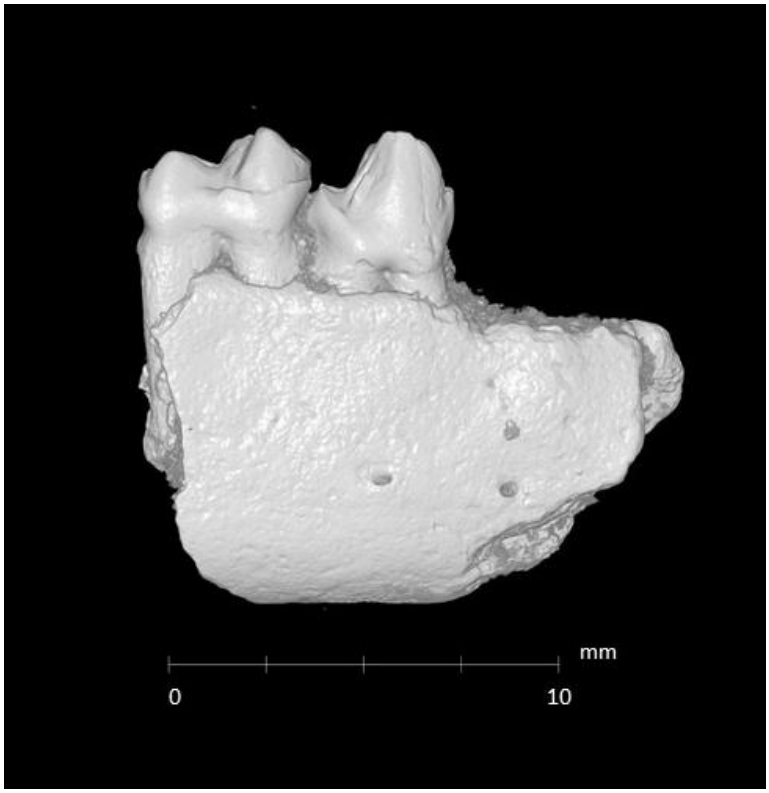

Figure 18. Lateral Surface of CM 95514, a *C. trigonodus* specimen with P_4 – M_1. Mesial to the right of the page.

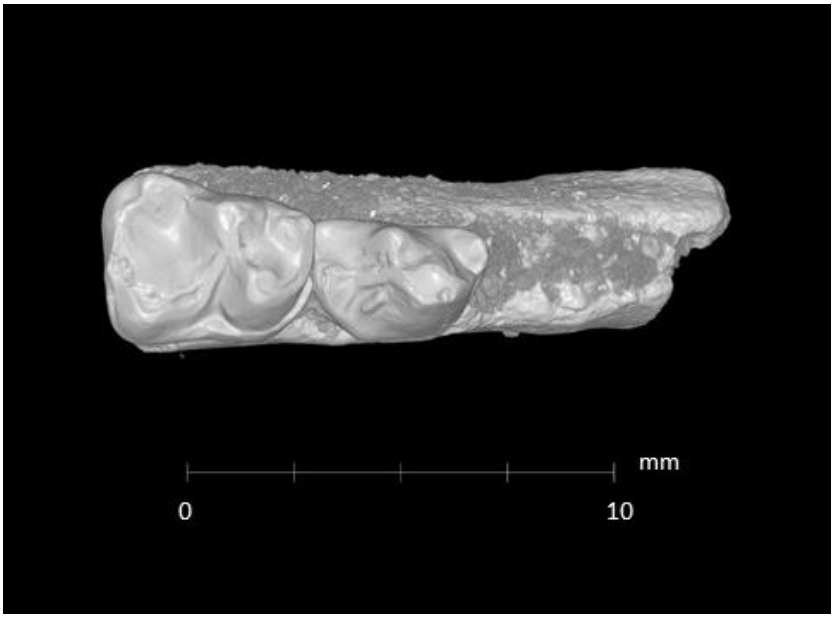

Figure 19. Occlusal Surface of CM 95514, a *C. trigonodus* specimen with P_4 – M_1. Mesial to the right of the page; buccal to the bottom of the page.

CM 95514 has been identified as a partial right mandible containing a fourth premolar and one molar, P_4-M_1. The premolar has paraconid, with a robust protoconid. The premolar shows evidence of molarization, as acknowledged in the description of CM 95513 (Figure 17). The M_1 has the signature trigonid created by the paraconid, metaconid, and protoconid. The talonid consists of the hypoconid, hypoconulid, and the entoconid. The hypoconulid is reduced significantly in this specimen, and the hypoconid is rather robust. Also, the talonid is elongated mesiodistally on the M_1, making it longer than the trigonid.

CM 95514 has not been previously identified at the species level, the specimen has only been placed into the genus *Cantius*. After reviewing the reconstructions (Figure 18-19) there were three significant dental characteristics that aided in the identification of this specimen. The first potentially diagnostic trait found in this specimen was the robust protoconid, the second trait is the reduced hypoconulid, and the final trait being the elongated talonid. These are all traits commonly observed in *C. trigonodus*. After considering these dental characteristics, it was evident to me that CM 95514 can be identified as *C. trigonodus.*

CM 95515

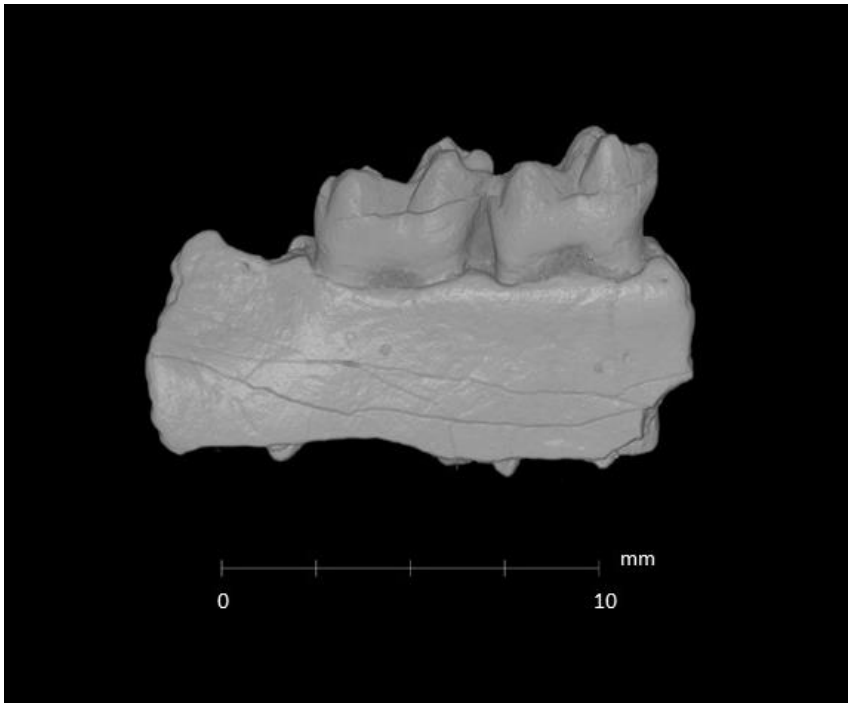

Figure 20. Lateral Surface of CM 95514, a *C. frugivorous* specimen with $M_1 – M_2$. Mesial to the right of the page.

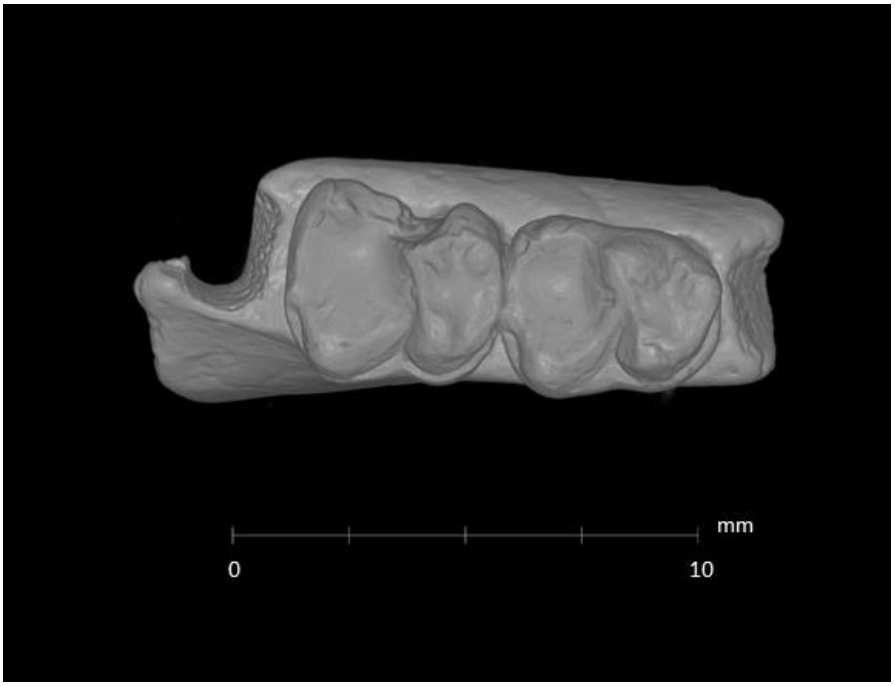

Figure 21. Occlusal Surface of CM 95515, a *C. trigonodus* specimen with $M_1 – M_2$. Mesial to the right of the page; buccal to the bottom of the page.

CM 95515 has been identified as a partial right mandible, consisting of two molars, M_1-M_2. The two molars both have the signature trigonid, consisting of a paraconid, metaconid, and protoconid. The metaconid on the M_1 is significantly reduced while the paraconid and protoconid are comparatively robust. On the other hand, the paraconid on the M_2 is reduced, while the protoconid maintains its robusticity (Figure 21). The talonid includes a hypoconulid, hypoconid, and entoconid, with evidence of an entoconid notch on both molars (Figure 20). The hypoconid appears to be robust, while the hypoconulid is much smaller, similar to the previous specimen, CM 95514 (Figure 19). The talonid is also elongated mesiodistally, a trait that has been observed in most of the other specimens.

CM 95515 has not been previously identified on the species level; the specimen has only been placed into the genus *Cantius*. There were three dental characteristics that were useful in classifying this specimen. The first characteristic being the robust trigonid cusps, the paraconid and the protoconid, a trait commonly observed in *C. frugivorous*. The second characteristic being the elongated talonid, another trait commonly observed in *C. frugivorous* and *C. trigonodus* (Beard, 1988; Covert 1990). The third characteristic used to aid in the species identification is the possible presence of the entoconid notches (O'Leary, 2021). After reviewing the reconstructions and considering the known biozone of Tim's Confession, I suggest that CM 95515 can be identified as *C. trigonodus*.

CM 95516

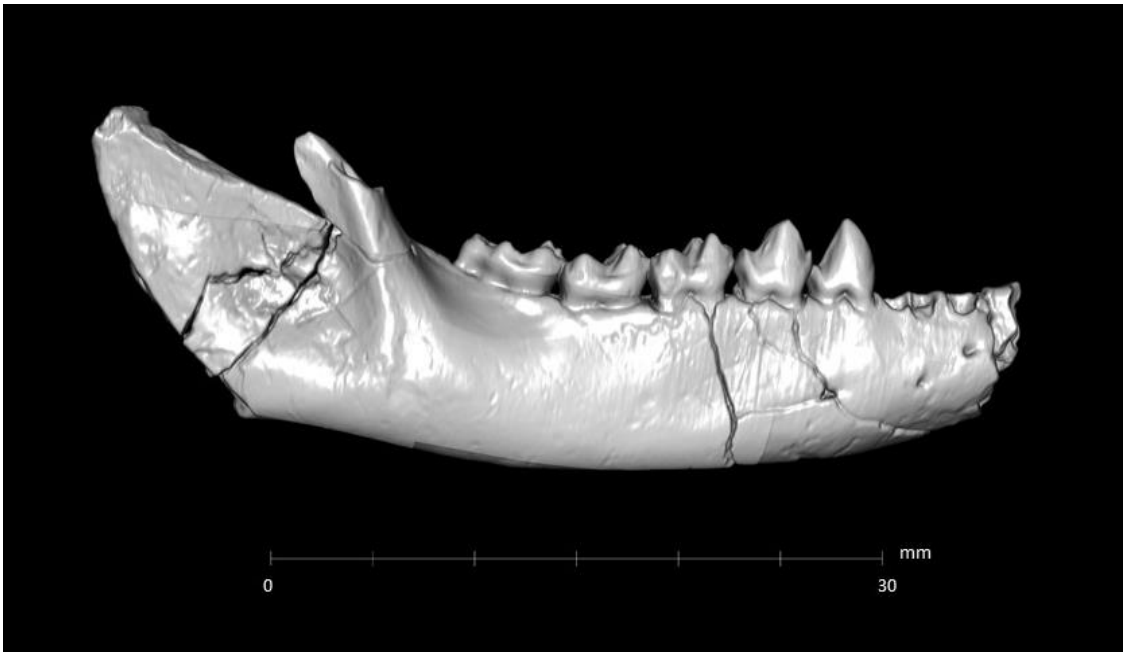

Figure 22. Lateral Surface of CM 95516, a *C. trigonodus* specimen with P_3 – M_3. Mesial to the right of the page.

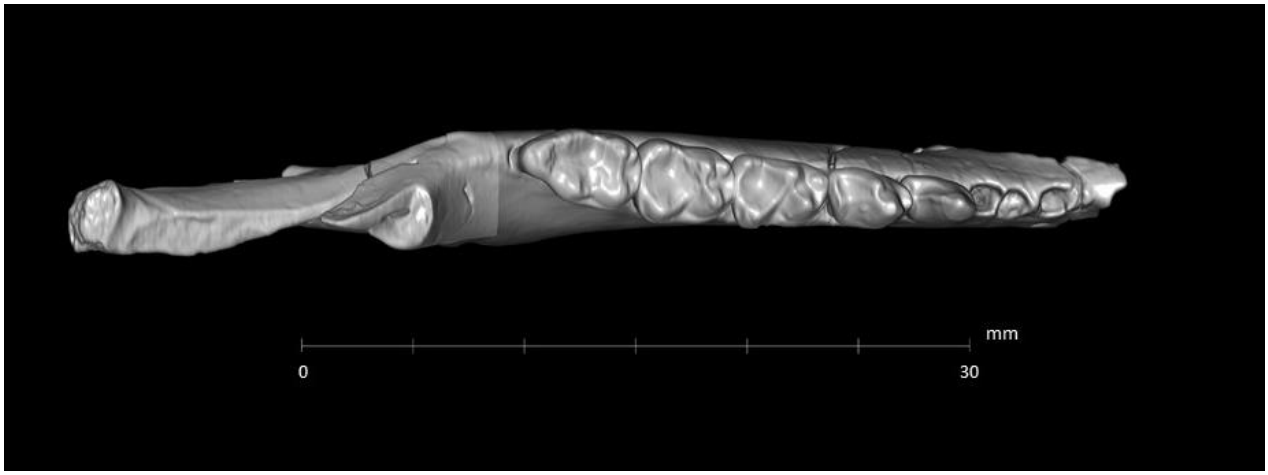

Figure 23. Occlusal Surface of CM 95516, a *C. trigonodus* specimen with P_3 – M_3. Mesial to the right of the page; buccal to the bottom of the page.

CM 95516 is one the most complete specimens in the collection. CM 95516 is a partial left mandible with two premolars and three molars, P_3-M_3. The P_3 has a robust protoconid. The P_4 has a single paraconid, a robust protoconid, and the P_4 also appears to possibly have a

slight metaconid towards the distal end of the tooth, which provides evidence for molarization (Figure 23). The molars have the signature trigonid including the paraconid, metaconid, and protoconid. The M_1 has a weak paraconid and a robust protoconid. On the M_2, the trigonid cusps are similar in size. However, the paraconid and the metaconid are very close together. This is also visible on the M_3, but the paraconid and metaconid are even closer. With the small trigonids, the talonid is longer mesiodistally. The talonid on the M_1 and M_2 are very similar, with a well-developed hypoconid, an entoconid, and a single hypoconulid. The M_1 and the M_2 also appear to be lacking an entoconid notch on the distal end of the tooth. The talonid on the M_3 is also well rounded, rather than squared.

CM 95516 has been previously identified as *C. trigonodus*. After further examination, I concur with the original classification based on the presence of molarization on the premolars, the elongated, well-rounded, talonid, and the lack of entoconid notches. While this specimen does have similar dental characteristics to *C. frugivorous*, based on the dates of the collection site and the lack of the entoconid notches I argue that this cannot be *C. frugivorous*. Therefore, I suggest that to initial classification was correct and that this specimen can be identified as *C. trigonodus*.

CM 95517

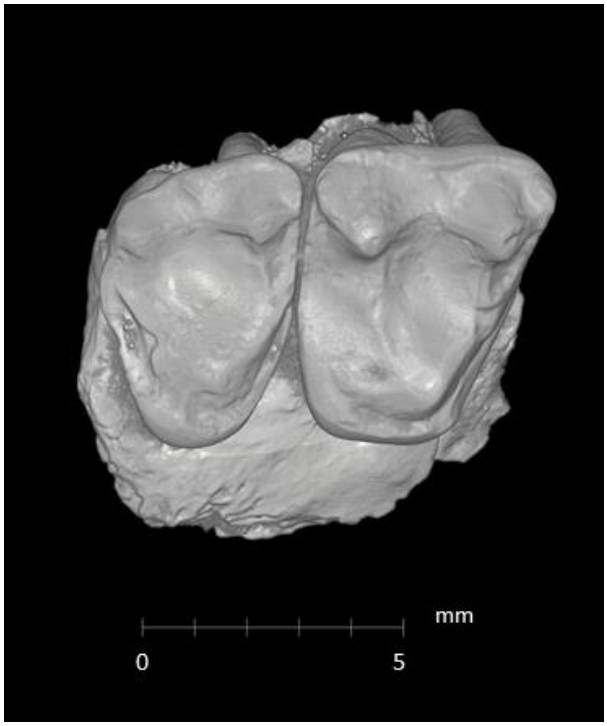

Figure 24. Occlusal Surface of CM 95517, a *C. trigonodus* specimen with M^2-M^3. Mesial to the right of the page; buccal to the top of the page.

CM 95517 has been identified as a partial right maxilla with two molars, M^2-M^3. The trigonids of both molars include a distinct paracone and metacone with a weaker protocone that appears to be more mesially positioned. However, the M^2 appears to be rather broad with the paracone and metacone positioned slightly further apart. The mesiocingulum and postcingulum have connected to form a continuous crest around the lingual portion of the tooth but the buccal cingulum is very weak on M^2 and does not appear to be present on the M^3. The Nannopithex-fold is also less developed on this specimen, and there does not appear to be evidence of a possible hypocone on either of the molars. The molars are also lacking strong styles, rather the styles on the molars are weak and less developed, a trait not commonly observed in *Cantius* species (Figure 24).

CM 95517 has been previously identified as *C. trigonodus*, however, there are not too many published details on the dental characteristics of *C. trigonodus* rather than the mentioning of the similarities between *C. trigonodus* and *C. frugivorous*. The dental morphologices described above are consistent with *C. frugivorous*. However, the lack of the buccal cingulum would suggest that this is an earlier species (O'Leary, 2021). It is possible that this specimen is a younger *C. trigonodus* specimen, but it is also possible that this specimen could be identified as *C. frugivorous*. It is difficult to definitively classify this specimen and thus I have decided to leave the species identification as it currently is.

CM 95509 – *Copelemur australotutus*

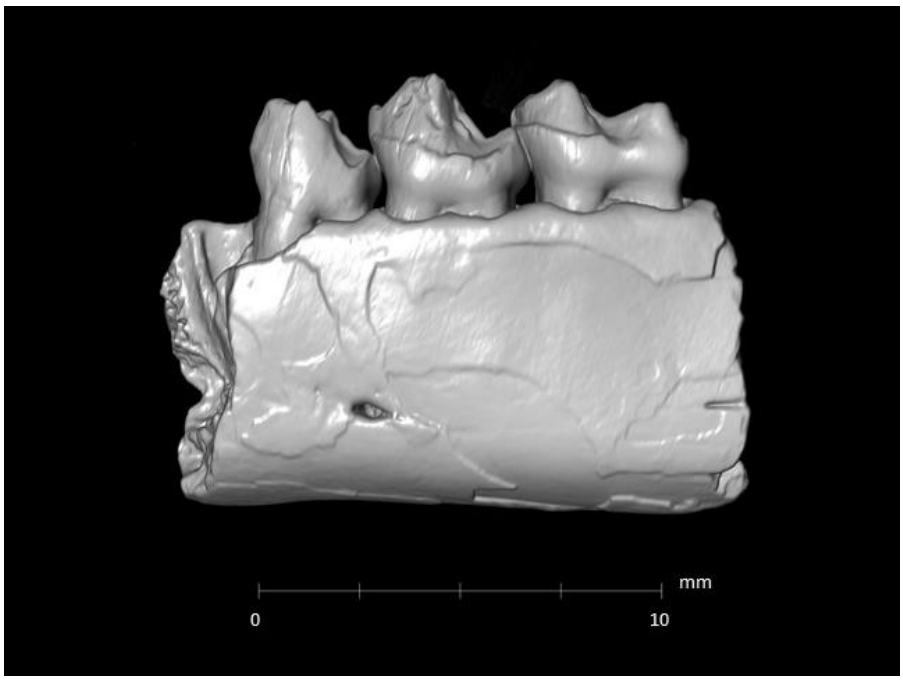

Figure 25. Lateral Surface of CM 95509, a *Copelemur australotutus* specimen with P_3 – M_1. Mesial to the left of the page.

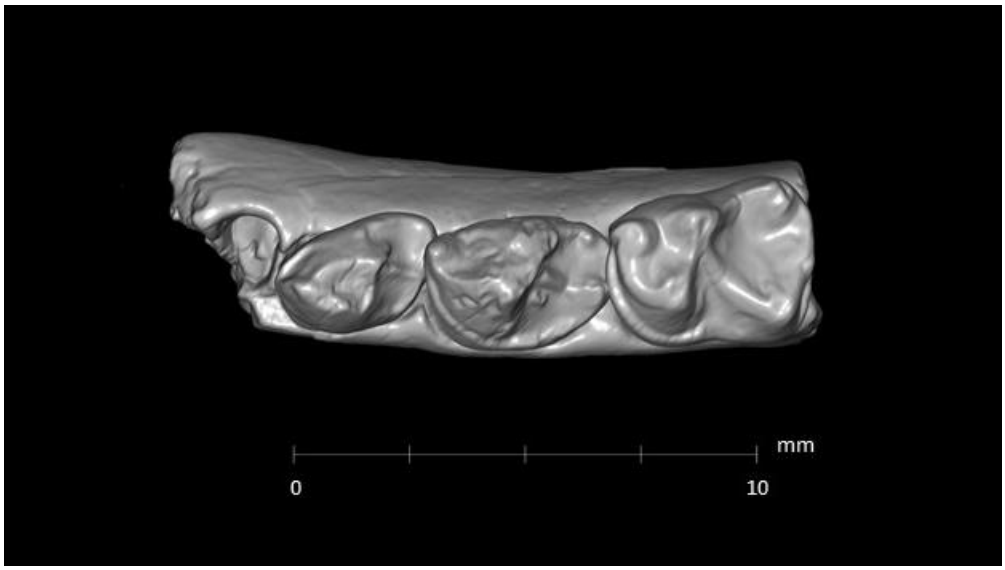

Figure 26. Occlusal Surface of CM 95509, a *Copelemur australotutus* specimen with P_3 – M_1. Mesial to the left of the page; buccal to the bottom of the page.

CM 95509 has been identified as a partial left mandible with two premolars and one molar, P_3-M_1. Both premolars consist of a paraconid, metaconid, protoconid, hypoconid, and the P_3 appears to have a hypoconulid. The paraconid on the P_4 appears to possibly have been twinned at some point, but due to the dental wear, this is unclear. The P_4 also appear to have evidence of molarization, exhibiting two distinct basins. The talonid on the premolars is smaller compared to the talonid on the molars. The molar, M_1, has the signature trigonid with a well-developed paraconid, metaconid, and protoconid. The talonid is slightly longer mesiodistally, as commonly noted in Notharctine primates. The talonid has a hypoconid, entoconid, and a diminutive entoconid. It appears there is an entoconid notch on the distal end of the M_1, however, the width of this notch is difficult to determine.

CM 95509 is the only *Copelemur* specimen scanned for this project. CM 95509 has been previously identified as *Copelemur australotutus*. The dental characteristics such as, the entoconid notch, and the size of the talonid on the premolars, and the possibility of twinned

paraconids, are consistent with the dental characteristics commonly observed in *Copelemur australotutus* (Beard, 1988; Gunnell, 2002). Unfortunately, we do not have any other *Copelemur* specimens scanned to use as a comparison and comparative data utilized for this study is derived from the literature. This complicates the identification of the specimen. Nonetheless, I have determined to that the specimen is *C. australotutus*.

Summary of Avizo reconstructions

Table 3 presents each specimen, its initial classification, and my re-classification. A justification for each re-classification is also provided in the last column.

Table 3. Summary of classifications of study specimens based on Avizo reconstructions.

Specimen	Classification	Re-classification	Justification
CM 93347	*Cantius frugivorous*	*Cantius frugivorous*	Strong Nannopithex-fold and slight mesostyle on M^2.
CM 93349	*Cantius frugivorous*	*Cantius frugivorous*	Presence of an entoconid notch, robust trigonid cusps, and elongated talonid.
CM 95510	*Cantius trigonodus*	*Cantius trigonodus*	Larger molar sizes, elongated talonid, and absence of entoconid notches.
CM 95511	*Cantius*	*Cantius trigonodus*	The elongated, rounded talonid, and the overall size of the M_2. The dates of the locality were used

			to identify this species as well due to the extreme wear on the molars.
CM 95512	*Cantius*	*Cantius trigonodus*	The closeness of the paraconid and the metaconid suggesting a shorter trigonid, the rounded talonid, and the single hypoconulid.
CM 95513	*Cantius*	*Cantius trigonodus*	Presence of a strong Nannopithex-fold, the crestifrom mesostyle and comparatively large M^2.
CM 95514	*Cantius*	*Cantius trigonodus*	Robust paraconid, reduced hypoconulid, and the elongated talonid.
CM 95515	*Cantius*	*Cantius trigonodus*	Robust trigonid cusps (paraconid and protoconid), elongated talonid, and possible presence of slight entoconid notches on both molars.
CM 95516	*Cantius trigonodus*	*Cantius trigonodus*	Evidence of molarization of P_4 lacking entoconid notches, and the elongated, well-rounded, talonid.
CM 95517	*Cantius trigonodus*	*Cantius trigonodus*	Weak styles, less developed protocone, and diminutive buccal cingulum.

CM 95509	*Copelemur australotutus*	*Copelemur australotutus*	Presence of an entoconid notch on the M_1, comparatively small talonid on premolars, and the evidence to suggest that there could have possibly been two, twinned paraconids on the premolars.

Molar measurements

Upper and lower molar measurements taken in Avizo of the eleven specimens are presented in Table 4. Additionally, the summary statistics of the 103 *Cantius* specimens measured using digital calipers are presented in Table 5.

Table 4. Molar measurements in millimeters of the study specimens.

Specimen	Molar(s)	Length (mm)	Width (mm)
CM 93347	M^1	3.68	4.70
	M^2	3.74	5.32
	M^3	3.32	4.66
CM 93349	M_1	3.95	3.10
CM 95510	M^2	4.36	3.58
CM 95511	M_2	4.29	3.60
	M_3	5.15	3.21
CM 95512	M_3	5.57	3.20
CM 95513	M^1	3.98	5.27
	M^2	4.06	5.39
	M^3	3.68	5.18

CM 95514	M_1	4.25	3.30
CM 95515	M_1	4.18	3.04
	M_2	4.16	3.55
CM 95516	M_1	3.95	3.03
	M_2	4.10	3.52
	M_3	5.15	3.15
CM 95517	M^2	4.29	3.60
	M^3	5.15	3.21
CM 95509	M_1	3.98	3.15

Table 5. Summary of molar measurements in millimeters including means, ranges, standard deviations, and coefficients of variation.

Tooth position	# of specimens	Mean (mm)	Range (mm)	S.D. (mm)	CV (mm)
M^1					
L	2	3.92	3.72-4.12	0.28	0.072
W		5.45	5.05-5.84	0.56	0.103
M^3					
L	13	3.32	2.95-3.76	0.28	0.084
W		5.06	4.60-5.71	0.35	0.068
M^u					
L	17	4.04	3.56-4.45	0.24	0.059
W		5.77	4.77-6.57	0.53	0.091
M_1					
L	19	4.34	3.89-4.71	0.18	0.042
W		3.27	2.70-3.72	0.25	0.076
M_2					
L	32	4.40	3.84-4.76	0.22	0.049
W		3.62	2.86-3.99	0.26	0.071
M_3					
L	19	5.21	4.76-5.64	0.25	0.048
W		3.20	2.41-3.52	0.27	0.084

M^1 = upper 1st Molar M^3= upper 3rd molar M^u = upper unknown molar M_1= lower 1st molar M_2 = lower 2nd molar M_3 = lower 3rd molar L = molar length W = molar width S.D. = standard deviation CV = coefficient of variation.

Chapter 5

Discussion and Conclusion

The three-dimensional dental morphology images of the *Cantius* and *Copelemur* specimens generated in this study largely align with the existing classifications proposed for the Notharctine primates described at Tim's Confession and North Hill. In essence, this study supports the existing alpha taxonomy of the Eocene primates at these sites. This study contributes to our understanding of Eocene primates overall and the genus *Cantius* more specifically. To begin with, the images generated from this study highlight some the similarities and differences in the dental morphology within the genus *Cantius* as evidenced in the variation revealed among the ten specimens examined here. Explanations for the variation revealed in this study are beyond the scope of this project. However, these differences may be linked to phylogenetic history, genetic or epigenetic factors, environmental selective factors, wear patterns linked to primate dietary regimes, or a combination of several of these variables.

Specimens collected from Tim's Confession

Eight of the specimens were collected from Tim's Confession and identified as *Cantius trigonodus* (CM 95510, CM 95511, CM 95512, CM 95513, CM 95514, CM 95515, CM 95516, and CM 95517). Four of the specimens examined for this study (CM 95510, CM 95514, CM 95516, CM 95517) were identifiable by the dental morphological traits displayed in the Avizo reconstructions. Specimens CM 95510, CM 95514, CM 95516 all include lower molars whereas CM 95517 consists of upper molars. The three of the specimens with lower molars show

evidence of an elongated talonid and lack entoconid notches on the molars, two traits commonly observed in *C. trigonodus* specimens (Beard, 1988; Covert, 1990). CM 99510 and CM 95514 each only consist of one molar each. However, CM 95516 includes all three molars. In comparison, the M_2 of 95510 and the M_2 of 95516 are similar in size. The M_1 of specimen CM 95514 is also similar to the M_1 of CM 95516 (Appendix 2). In addition, the overall size of the molars on all three of these specimens align closely with the other 103 *Cantius trigonodus* specimens that were measured as part of this project (Appendix 1).

CM 95517 was slightly more difficult to identify. However, after close examination of the dental morphology and the consideration of the dates of Tim's Confession and the molar measurements confirm that this specimen belongs to *C. trigonodus.* CM 95517 includes the upper molars, therefore, the basic morphology of the teeth is different from that of CM 95510, CM 95514, and CM 95516. The diagnostic dental characteristics for CM 95517 include the presence of a Nannopithex-fold, the lack of a buccal cingulum on the M_3, and the less developed styles. These are traits commonly observed in both *C. trigonodus* and *C. frugivorous* specimens (Beard, 1988; Covert, 1990). While these two species have similar dental morphology, the overall size of the teeth and the known age of these two species are different. *C. trigonodus* is known to date to Wa4 similar to Tim's Confession, while *C. frugivorous* is suggested to date to Wa6. Interestingly, *C. frugivorous* is the only *Cantius* species that is known to have decreased in size. This resulted in the molars also decreasing in size. The molars on CM 95517 are consistent with the upper molar measurements of *Cantius trigonodus* (Appendix 1). After considering these factors, I suggest that the classification remain, supporting the existing taxonomy.

While the classifications of CM 95510, CM 95514, CM 95516, and CM 95517 were slightly easier to determine, the remaining four specimens collected from Tim's Confession (CM

95511, CM 95512, CM 95513, and CM 95515) were more difficult. For example, CM 95511 and CM 95512 in particular show evidence of extreme dental wear, which acted as a challenge when attempting to determine the species level classification of these two specimens. CM 95511 includes the M_2 and M_3, however, the M_2 is significantly misplaced which makes this specimen rather interesting. This misplacement of the M_2 appears to have impacted the wear patterns on the M_3, making the dental characteristics difficult to classify. Based on only dental morphology, this specimen appears to exhibit dental characteristics more aligned with *C. mckennai*, an older species from bizone Wa3 (Gunnell, 2002). The evidence of pitting present on the M_3 of CM 95511, resembles two hypoconulids present at one point in time, a trait specific to *C. mckennai* (Beard, 1988). However, the measurements of the molars on CM 95511 are similar to the measurements of *C. trigonodus* (Appendix 1; Table 4). It is also important to note that Tim's Confession has been placed in the Wa4 biozone, and the only *Cantius* species known to have existed during the same biozone is *C. trigonodus* (Gunnell, 2002), which further supports the existing classification of this specimen.

The molars of CM 95512 and CM 95511 shows evidence of dental wear. CM 95512 consists of only one molar, the M_3. Based on the wear patterns present on this specimen, the cusps that constitute the talonid very difficult to clearly identify. This resulted in complications when attempting to determine the taxonomic classification of this specimen. The lack of the cusps indicate that this specimen could potentially be *C. ralstoni*, an older species from biozone Wa1 (Gunnell, 2002). However, it is implausible to suggest that CM 95512 belongs to *C. ralstoni* given the known stratigraphic position of this specimen at Tim's Confession. Further, the measurements of this M_3 are also closely aligned with the measurements of *C. trigonodus* specimens (Appendix 1; Table 4).

CM 95513 is one of the most complete specimens with five teeth in total, $P^3 – M^3$. The dental morphological traits of the teeth on this specimen are traits commonly observed throughout the entire genus, which makes it difficult to determine exactly which species this specimen belongs to based simply on the dental morphology shown in the reconstructions (Beard, 1988; O'Leary, 2021). This specimen was classified simply by considering the dates of Tim's Confession and the overall size of the molars. While only an additional 17 *C. trigonodus* upper molars were measured, the measurements of the molars on CM 95513 seem to align with the measurements of the other 17 specimens. Without the measurements of the molars, the classification of CM 95513 would have been incredibly difficult to determine (Appendix 1; Table 4).

Finally, CM 95515 is an interesting specimen because the dental morphology is more similar to the genus *Copelemur*, another Notharctine genera. The main similarity between CM 95515 and *Copelemur* is what appears to be early evidence of an entoconid notch on the most distal end of the molar near the hypoconulid (Beard, 1988; Covert, 1990; O'Leary, 2021). The only documented evidence of an entoconid notch in the genus *Cantius* is found among *C. frugivorous*. However, *C. frugivorous* does not appear in the fossil record until the Wa6 biozone (Gunnell, 2002). Interestingly, the first *Copelemur* species make their appearance in the fossil record during Wa4, similar to *C. trigonodus*. Unfortunately, the sample size for this project is comparatively small, and there is only one other *Copelemur* specimen to compare CM 95515 to, therefore, I am lacking the dataset required to justifiable re-classify this specimen. The molar measurements of CM 95515 align with the measurements *C. trigonodus* (Appendix 1; Table 4), which in combination with the lack of comparison data, re-affirms the initial classification.

The molar measurements collected for this study provided quantitative data that could be compared to published accounts of *Cantius*. These data were imperative for the classification of the specimens collected from Tim's Confession. The morphological reconstructions generated from of the specimens included in this study are largely qualitative, and among the specimens there was a fair degree of variation among the dental traits analyzed here. Without the inclusion of the molar measurements (i.e. quantitative data) and 3-dimensional scans (i.e. qualitative data) many of the specimens examined in this study would have been misidentified.

Specimens collected from North Hill

Three of the specimens selected for this project were collected from North Hill. These include CM 93349 which was collected from North Hill 7185; CM 93347 which was collected from Hill 7125 and CM 95509 which was collected from Scorpio. To date, the three localities have not been assigned an exact biozone. However, all three sites are known to be part of the Wasatchian North American Land Mammal Age (Woodbourne, et. al., 2009).

CM 93347 and CM 93349 have both been identified as *C. frugivorous* specimens. CM 93347 consists of upper molars, the M^1 – M^3, with characteristics such as a strong Nannopithex-fold and a slight mesostyle on the M^2, traits commonly observed in *C. frugivorous* specimens. The measurements of the molars on CM 93347 would also suggest that the molars were slightly smaller than *C. trigonodus*, further supporting the existing classification given the fact that *C. frugivorous* is known to have been smaller than *C. trigonodus* (Beard, 1988; Covert, 1990). CM 93349 consists of one lower molar, the M_1, with characteristics such as the diagnostic entoconid notch, the robust trigonid cusps (paraconid, metaconid, and protoconid), and the elongated talonid. The entoconid notch present on the M_1 and the robust trigonid cusps are traits commonly

observed in *C. frugivorous* specimens (Beard, 1988; Covert, 1990; O'Leary 2021). In addition, the measurements of the molar on CM 93349 appears to be smaller in comparison to *C. trigonodus* (Appendix 1; Appendix 2). Therefore, the morphometric data would suggest that the existing classification is correct.

CM 95509 has been previously identified as *Copelemur australotutus*. CM 95509 is the only specimen in this project that has not been classified into the genus *Cantius*. CM 95509 was added to the project as a source of comparison. However, this specimen appears to lack some of the diagnostic traits associated with the genus *Copelemur* (Beard, 1988). For example, CM 95509 does not appear to have entoconid notches, a trait that has been observed in *Copelemur* specimens (Covert, 1990). This makes this specimen difficult for comparisons to dental morphology of *Cantius*. The molar measurements of CM 95509 are similar to *C. australotutus* and *C. frugivorous* (Appendix 1; Table 4). The similarities between these two species encouraged me to agree with the existing classification.

Comparison to extant Malagasy lemurs

Given the small sample size of the *Cantius* specimens analyzed for this study direct comparisons of *Cantius* to the extant Malagasy lemurs are difficult and untenable. However, the three-dimensional reconstructions displaying the dental morphology of the *Cantius* specimens and molar measurements analyzed do allow for initial observations regarding the potential relationships between *Cantius* and modern-day lemurs of similar body.

Dental Morphology

One of the common similarities observed in *Cantius* specimens and extant lemur species is the overall shape of the premolars. While this study sample is comparatively small, with only four specimens consisting of premolars, three out of these four specimens display premolar morphology similar to extant lemur species. The P_3 in extant lemurs appear to be canine-like, and this trait can be observed in one of the study specimens, CM 93349 (Figure 9). The P_4 in extant lemurs show evidence of molarization. The molarization of the premolars is characterized by the development two distinct basins on the P_4 (Cuozzo and Yamashita, 2012; Gebo, 2014). Two of the study specimens also display this characteristic, CM 95514 (Figure 19) and CM 95516 (Figure 23).

Another diagnostic trait that is commonly observed in both *Cantius* and most extant lemur species is the shape of the upper molars. The upper molars in both groups are triangular in shape, with three distinct cusps known as the metacone, paracone, and protocone (Figure 8; Figure 17; Figure 24) (Covert, 1990; Cuozzo and Yamashita, 2012). However, the largest of the Malagasy lemurs, the Indri, has a fourth cusp referred to as the hypocone, changing the triangular maxillary molar to be more quadritubercular in shape (Cuozzo and Yamashita, 2007). Interestingly, some *Cantius* specimens are known to have developed a weaker fourth cusp as well, and this is referred to as a "pseudohypocone" (Beard, 1988; Covert, 1990). Unfortunately, this study sample does not include a specimen with a "pseudohypocone." However, the occasional presence of a "pseudohypocone" in the genus *Cantius* is well documented in the literature (Beard, 1988; Covert, 1990; O'Leary, 2021). This could suggest that the "pseudohypocone" developed further into a definitive fourth cusp, similar to what is present in Indris.

The lower molars of Malagasy lemurs, however, are comparatively different from the specimens examined for this study. The primary difference between these two groups is the lack of paraconids and hypoconulids in Malagasy lemurs, two cusps that are present in the lower molars of *Cantius* (Beard. 1988; Cuozzo and Yamashita, 2012). All of the study specimens had well-developed paraconids. However, there were several specimens with weak hypoconulids (CM 95510, CM 95511, CM 95512, CM 95513, and CM 95515). The less developed hypoconulids present in some of the specimens could suggest that the hypoconulids were no longer being selected for within the genus *Cantius*, similar to the extant Malagasy lemurs.

Molar Measurements

The molar measurements of the *Cantius trigonodus* specimens align with the molar measurements of *Lemur catta* (Appendix 3). The molar measurements for *Lemur catta* are slightly smaller than the measurements of the *Cantius* specimens, which is consistent with the slight difference in body size observed in these two groups of primates. *Lemur catta* is known to be around 2.2 kg, while *Cantius* specimens are hypothesized to be anywhere from 3 to 3.5 kg (Fleagle, 2013). However, the genus *Cantius* underwent a series of weight changes throughout its' evolutionary history with the earliest species being roughly 1 kg and the later species reaching almost 4 kg (Fleagle, 2013; Beard, 1988). Therefore, the body size of *Cantius* is difficult to use for comparison purposes, which encourages the use of the molar measurements for a better comparative study. A larger study sample and further statistical analysis is needed in order to conduct a direct comparison, however, the data generated from this project has made it possible to hypothesize that *Lemur catta* and *Cantius* have similar molar and body sizes.

Future Research

While this project relied primarily on the fossil remains of ten *Cantius* specimens, future improvements of this study would include a larger sample size including both three-dimensional reconstructions generated by Avizo and molar measurements of each *Cantius* specimen. Further statistical analyses of *Cantius* molar measurements would be beneficial, along with more specimens of other Notharctine genera for further comparison. An enhanced version of this study would also benefit from the inclusion of a more extensive analysis of modern strepsirrhine primate dental morphology, which would include the molar measurements of several different strepsirrhine primate species to be used for comparison. While this project contributed a number of useful reconstructions to this study, more dental, cranial, and post cranial data are required to fully understand the taxonomy of *Cantius*, and the relationship this genus has with other extinct and extant primates.

REFERENCES

Anemone, Robert L., Nachman, Brett. 2017. North American Primate Fossil Record. *The International Encyclopedia of Primatology.* James Wiley and Sons, Inc.

Anemone, Robert L., Skinner, Matthew M., Dirks, Wendy. 2012. Are there two distinct types of hypocone in the Eocene primates? The "pseudohypocone" of Notharctines revisited. *Palaeontologia Electronica*, 15(3).

Beard, K. Christopher. 1988. New Notharctine Primate Fossils from the Early Eocene of New Mexico and Southern Wyoming and the Phylogeny of Notharctinae. *American Journal of Physical Anthropology*, 75: 439-469.

Beard, K. Christopher. 2008. The oldest North American primate and mammalian biogeography during the Paleocene-Eocene Thermal Maximum. *PNAS*, 105(10): 3815-3818.

Berthaume, Michael A., Lazzari, Vincent, Guy, Franck. 2020. The landscape of tooth shape: Over 20 years of dentaltopography in primates. *Evolutionary Anthropology*, 29: 245 – 262.

Bown, T.M., Beard, K.C. 1990. Systematic lateral variation in the distribution of fossil mammals in alluvial paleosols, lower Eocene Willwood Formation, Wyoming. *Dawn of the Age of Mammals in the Northern Part of the Rocky Mountain Interior, North America: Geological Society of America Special Paper*, 243: 135-151.

Covert, Herbert H. 1990. Phylogenetic Relationships Among the Notharctinae of North America. *American Journal of Physical Anthropology*, 81: 381-397.

Cunningham, John A., Rahman, Imran A., Lautenschlager, Stephan, Rayfield, Emily J., Donoghue, Philip C.J. 2014. A virtual world of paleontology. Trends in Ecology and Evolution, 29(6): 347-357.

Cuozzo, Frank P., Yamashita, Nayuta. 2006. Impact of Ecology on the Teeth of Extant Lemurs: A Review of Dental Adaptations, Function, and Life History. In: Gould, L., Sauther, M.L. (eds) Lemurs. Developments in Primatology: Progress and Prospect. *Springer*, Boston, MA.

Cuozzo, Frank P., Unagar, Peter S., Sauther, Michelle L. 2012. Primate Dental Ecology: How Teeth Respond to the Environment. *American Journal of Physical Anthropology*, 148: 159-162.

Fleagle, John G. 2013. *Primate Adaptation and Evolution*. Academic Press: San Diego, California.

Gebo, Daniel L., Dagosto, Marian, Rose, Kenneth D. 1991. Foot Morphology and Evolution in Early Eocene *Cantius*. *American Journal of Physical Anthropology*, 86: 51-73.

Gebo, Daniel C. 2014. *Primate Comparative Anatomy*. John Hopkins University Press: Baltimore, Maryland.

Gingerich, Philip D. 2006. Environment and evolution through the Paleocene-Eocene Thermal Maximum. *Science Direct*, 21(5).

Gingerich, Philip D. 2003. Mammalian responses to climate change at the Paleocene-Eocene boundary: Polecat Bench record in the norther Bighorn Basin, Wyoming. *Geological Study of America (Special Paper 369*), 463-478.

Gingerich, Philip D., Simons, E.L. 1977. Systematics, phylogeny, and evolution of the early Eocene Adapidae (Mammalia, Primates) in North America. Contributions from the Museum of Paleontology, The University of Michigan 24(22): 245-279.

Gingerich, Philip D., Schoeninger, Margaret J. 1979. Patterns of tooth size variability in the dentition of primates. *American Journal of Physical Anthropology*, 51: 457-466.

Gingerich, Philip D., Smith, Holly B., Rosenberg, Karen. 1982. Allometric Scaling in the Dentition of Primates and Prediction of Body Weight from Tooth Size in Fossils. *American Journal of Physical Anthropology*, 58: 81-100.

Gingerich, Philip D., Haskin, R.A. 1981. Dentition of early Eocene *Pelycodus jarrovii* (Mammalia, Primates) and the generic attribution of species formerly referred to *Pelycodus*. *Contributions from the Museum of Paleontology, The University of Michigan*, 25: 327-337.

Gingerich, Philip D., Ryan, Alan S. Dental and Cranial Variation in Living Indriidae. *Primates*, 20(1): 141-159.

Gunnell, Gregg F. 2002. Notharctine primates (Adapiforms) from the early to middle Eocene (Wasatchian-Bridgerian) of Wyoming: transitional species and the origins of *Notharctus* and *Smilodectes*. *Journal of Human Evolution*, 43: 353-380.

Hyland, Ethan., Sheldon, Nathan D., Fan, Majie. 2013. Terrestrial paleoenvironmental reconstructions indicate transient peak warming during the early Eocene climatic optimum. *Geological Society of America*, 125(7): 1338-1348.

Inglis, Gordon N., et. al. 2020. Global mean surface temperature and climate sensitivity of the early Eocene Climatic Optimum (EECO), Paleocene-Eocene Thermal Maximum (PETM), and latest Paleocene. *Clim. Past*, 16: 1953-1968.

Kay, Richard F. 1975. The Functional Adaptations of Primate Molar Teeth. *American Journal of Physical Anthropology*, 43: 195-216.

Lautenschlager, Stephan. 2016. Reconstructing the past: methods and techniques for the digital restoration of fossils. *Royal Society Open Science*, 3:160342.

Mayr, Ernst. 1982. *The Growth of Biological Thought: Diversity, Evolution, and Inheritance*. The Belknap Press of Harvard University Press, Cambridge, Massachusetts.

Mayr, Ernst. 1963. The Taxonomic Evaluation of Fossil Hominids. *Classification and Human Evolution,* Routledge.

Ravosa, Matthew J. 1996. Mandibular form and function in North American and European Adapidae and Omomyidae. *Journal of Morphology*, 229: 171-190.

Rose, Kenneth D. and Walker, Alan. 1985. The skeleton of early Eocene *Cantius*, oldest lemuriform primate. *American Journal of Physical Anthropology*, 66: 73-89.

Rose, K.D., Macphee, R.D.E., and Alexander, J.P. 1999. Skull of early Eocene *Cantius abditus* and its phylogenetic implications, with a reevaluation of "*Hesperolemur" actius*. *American Journal of Physical Anthropology*, 109: 523-539.

Sauthers, Michelle L., Cuozzo, F.P., Sussman, R.W. 2001. Analysis of Dentition of a Living Wild Population of Ring-Tailed Lemurs (*Lemur catta*) From Beza Mahafaly, Madagascar. *American Journal of Physical Anthropology*, 114: 215-223.

Silcox, Mary T., Rose, Kenneth D., Bown, Thomas M. 2008. Early Eocene Paromomyidae from the Southern Bighorn Basin, Wyoming: Systematics and Evolution. *Journal of Paleontology*, 82(6): 1074-1113.

Uldin, Tanya. 2017. Virtual anthropology – a brief review of the literature and history of computed tomography. *Forensic Sciences Research*, 2(4): 165-173.

Ungar, Peter. 1998. Dental Allometry, Morphology, and Wear as Evidence for Diet in Fossil Primates. *Evolutionary Anthropology*, 205-217.

Weber, Gerhard W. 2015. Virtual Anthropology. *Yearbook of Physical Anthropology*, 156: 22-42.

Wilson, E. O. 2010. The major historical trends of biodiversity studies. *Systema Naturae 250—The Linnaean Ark*, CRC Press.

Woodbourne, Michael O., Gunnell, Gregg F., Stucky, Richard K. 2009. Climate directly influences Eocene mammal faunal dynamics in North America. *PNAS*, 106(32): 13399-13403.

Yamashita, Nayuta. 1997. Molar morphology and variation in two Malagasy lemur families (Lemuridae and Indriidae). *Journal of Human Evolution*, 35: 137-162.

APPENDIX 1

M^1 Measurements

GDB Project #	Length (mm)	Width (mm)
13600	5.05	3.72
12015	5.84	4.12

M^3 Measurements

GDB Project #	Length (mm)	Width (mm)
9850	5.07	3.69
10042	5.53	3.37
10045	4.80	3.00
10105	4.60	3.00
10106	5.00	3.76
10517	5.04	3.09
11011	5.06	3.26
11341	4.72	3.40
11342	5.05	3.13
12027	4.77	3.57
13250	5.58	3.27
13251	5.71	3.64
13580	4.88	2.95

M^u (u = unknown position) Measurements

GDB Project #	Length (mm)	Width (mm)
9923	5.76	4.10
9943	6.42	4.29
9945	5.35	3.67
9972	4.94	3.86
10036	4.77	3.56
10038	5.80	3.89
10040	6.05	3.94
10043	5.43	4.11
10461	6.17	3.99
11010	5.95	4.45
11334	6.57	4.07
11410	5.94	4.08
11934	6.45	4.43
12016	5.55	3.84
12480	5.97	4.17
13237	5.87	4.18
13244	5.03	4.04

M_1 Measurements

GDB Project #	Length (mm)	Width (mm)
8884	4.43	3.41
9225	4.47	3.44
9922	4.32	3.05
9924	4.22	3.41
9925	4.71	3.35
9926	4.48	3.72
9927	4.28	3.40
9944	4.01	3.26
10107	4.41	3.00
10108	4.52	3.70
10457	4.53	3.24
10458	4.30	3.04
11009	4.38	3.35
12013	4.34	3.26
12021	4.41	3.32
12028	4.29	2.99
12043	3.89	2.70
12120	4.25	3.14
12186	4.30	3.40

M_2 Measurements

GDB Project #	Length (mm)	Width (mm)
8861	4.61	3.99
9242	4.44	3.85
9243	4.55	3.69
9928	4.50	3.29
9929	4.68	3.87
9930	4.30	3.82
9931	4.62	3.80
9932	4.28	3.59
9933	4.30	3.83
9934	4.61	3.52
9935	4.30	3.50
9936	4.09	3.33
9938	4.00	3.56
9939	4.13	3.45
9940	4.24	3.71
9941	4.42	3.46
9950	4.43	3.62
10459	4.59	3.53
11006	4.55	3.36
11183	4.30	3.24
11184	4.76	3.92

11325	4.45	3.81
11326	4.53	3.89
12018	4.47	3.62
12020	3.84	3.21
12022	4.41	3.79
12024	4.04	3.78
12030	4.65	3.97
12109	4.17	3.63
12120	4.42	3.56
12510	4.46	3.84
13200	4.55	2.86

M_3 Measurements

GDB Project #	Length (mm)	Width (mm)
8903	5.54	3.46
9240	5.20	3.20
9910	4.95	3.15
9911	5.19	3.28
9912	5.31	3.16
9913	5.08	3.18
9917	5.29	3.08
9919	4.94	2.41
9920	5.37	3.50

9921	5.56	3.52
9939	5.43	3.38
10460	5.41	3.14
11185	5.37	3.49
11312	4.98	2.86
11313	5.04	3.07
12023	5.64	3.50
12120	5.09	3.27
12518	4.76	3.15
12519	4.91	3.02

APPENDIX 2

Scatter Plots of the Molar Measurements

Upper Molars

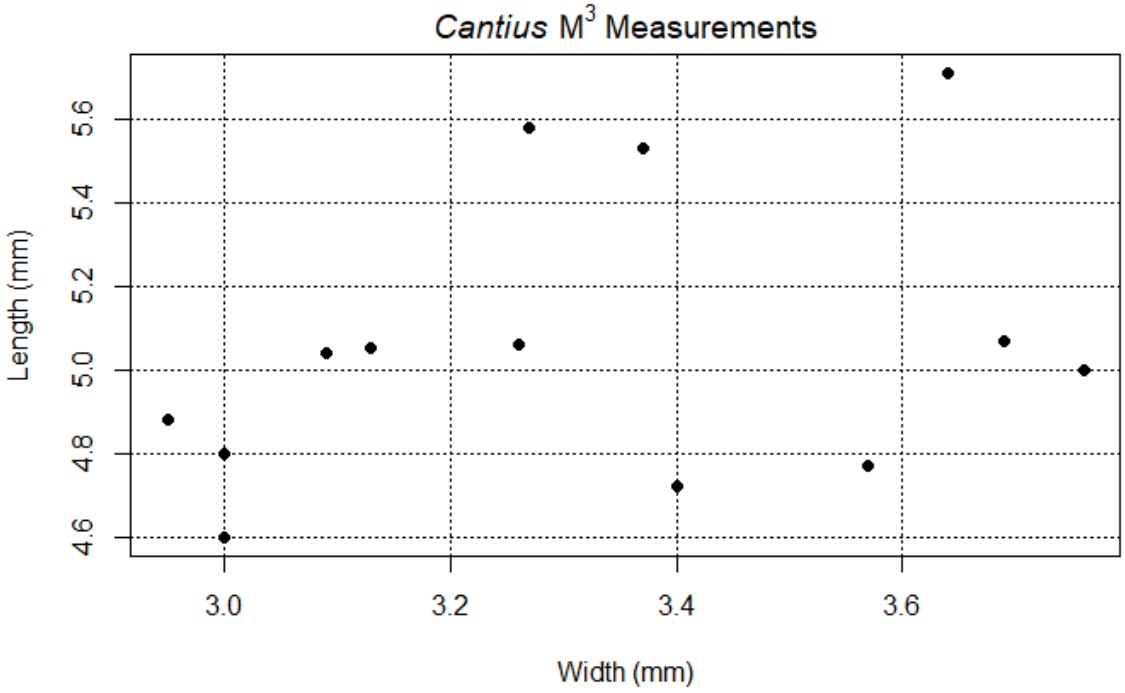

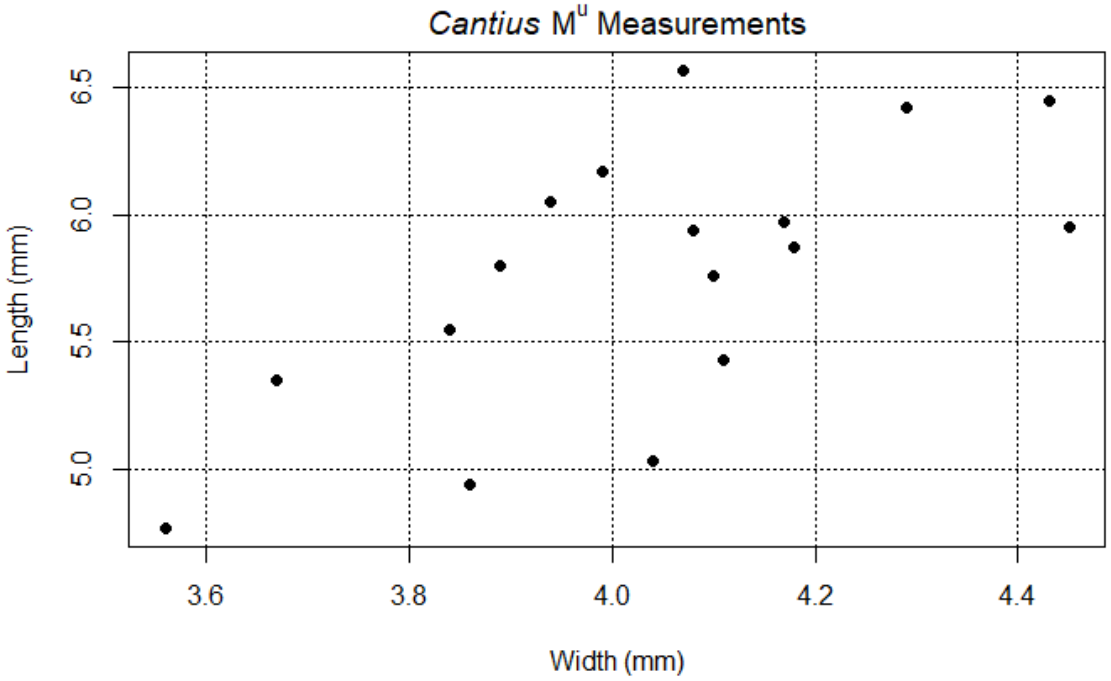

Lower Molars

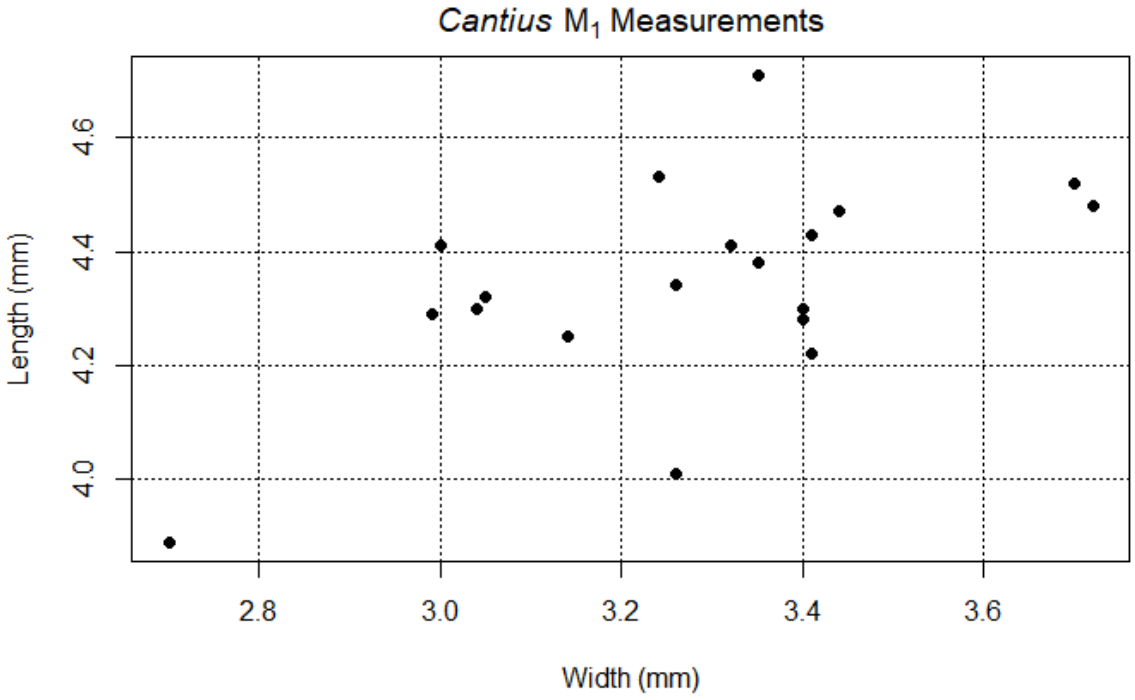

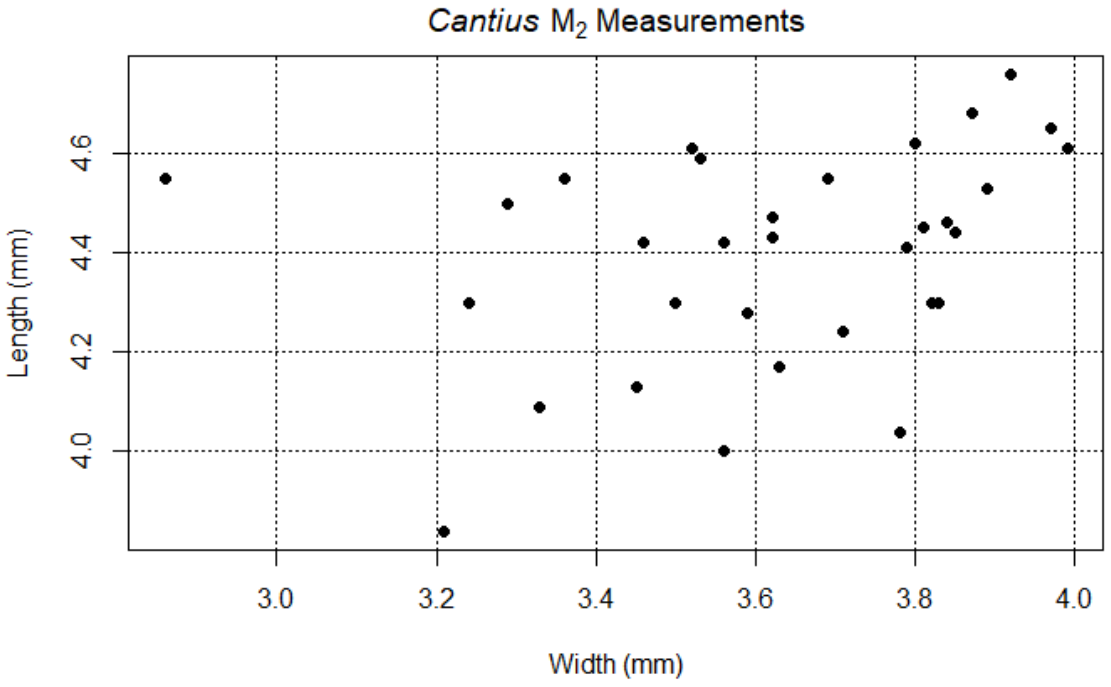

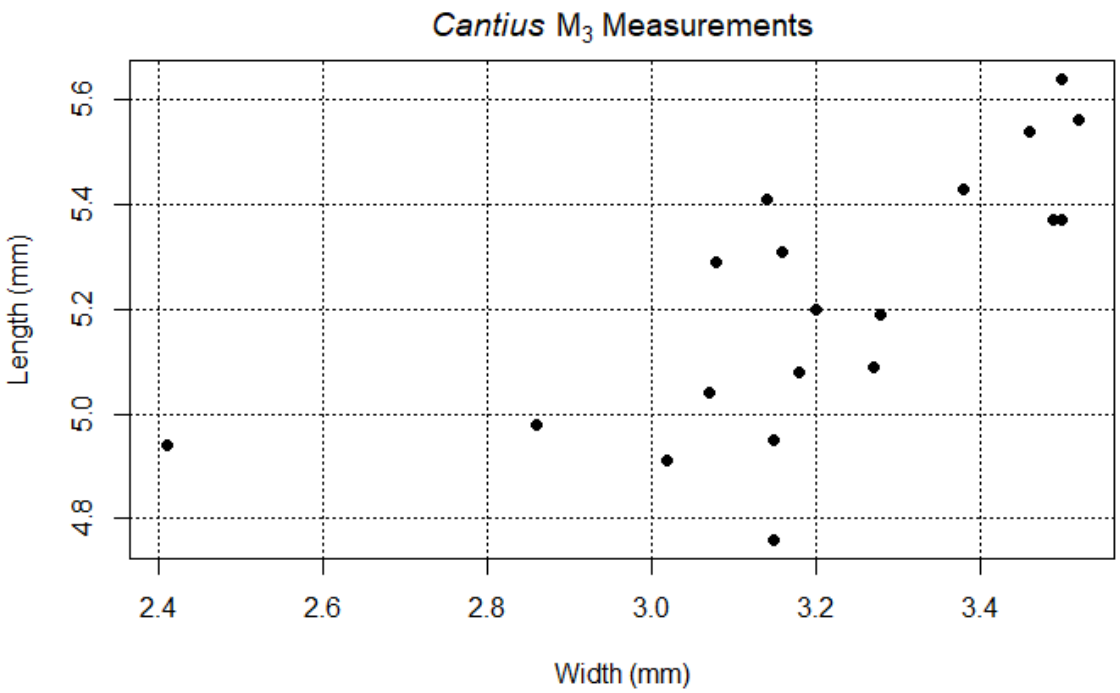
Cantius M_3 Measurements
Length (mm)
4.8
5.0
5.2
5.4
5.6
2.4
2.6
2.8
3.0
3.2
3.4
Width (mm)

APPENDIX 3

Molar Measurement Means of *Lemur catta*

Molar	Length (mm)	Width (mm)
M^1	4.62	5.76
M^2	5	6.42
M^3	4.94	5.19
M_1	4.71	3.29
M_2	5.10	3.61
M3	5.14	3.31